Electronic supplementary information

Trithiazolyl-1,3,5-triazines bearing decyloxybenzene moieties: synthesis, photophysical and electrochemical properties, as well as self-assembly behavior

Shin-ichiro Kato,[a‡] Satoshi Jin,[a] Terutaka Kimura,[a] Naoki Yoshikawa,[a]
Daiki Nara,[a] Kenji Imamura,[b] Yoshihito Shiota,[b] Kazunari Yoshizawa,[b]
Ryo Katoono,[c] Takeshi Yamanobe,[a] Hiroki Uehara,[a] and Yosuke Nakamura*[a]

[b] *Division of Molecular Science, Faculty of Science and Technology, Gunma University, 1-5-1 Tenjin-cho, Kiryu, Gunma 376-8515, Japan*
[c] *Institute for Materials Chemistry and Engineering, Kyushu University, 744 Motooka, Nishi-ku, Fukuoka 819-0395, Japan*
[d] *Department of Chemistry, Faculty of Science, Hokkaido University, Kita 10, Nishi 8, Kita-ku, Sapporo 060-0810, Japan*
‡ *Present address: Department of Materials Science, School of Engineering, The University of Shiga Prefecture, 2500 Hassaka-cho, Hikone, Shiga 522-8533, Japan*

Table of Contents

1. General experimental methods

Commercially available reagents were used as received. Et_2O, THF, CH_2Cl_2, and *o*-dichlorobenzene (*o*-DCB) were distilled from relevant drying agents prior to use. A fresh lithium diisopropylamide (LDA) was prepared as follows: a solution of *N*,*N*-diisopropylamine (1.0 mL, 14.1 mmol) in THF (10 mL) was added dropwise to a *n*-BuLi hexane solution (2.66 mol L^{-1}, 5.6 mL, 14.9 mmol) at −78 °C under argon atmosphere, and then the resulting mixture was stirred at −78 °C for 1 h and at 0 °C for 1 h. Boronic acid pinacol ester **9**[1] and 1-decyloxy-4-ethynylbenzene[2] were known compounds. Column chromatography and plug filtrations were carried out with SiO_2. Thin layer chromatography (TLC) was conducted on aluminum sheets coated with SiO_2; visualization with a lamp (254 or 365 nm). Melting points (M.p.) were measured with a hot-stage apparatus and are uncorrected. ^1H NMR and ^{13}C NMR spectra were recorded in $CDCl_3$ at 298 K. Residual and deuterated solvent signals in the ^1H and ^{13}C NMR spectra were used as an internal reference, respectively ($CDCl_3$, ^1H: δ 7.26; ^{13}C: δ 77.16). Chemical shifts (δ) are given as δ values. The coupling constants (*J*) are given in Hz. The apparent resonance multiplicity is described as s (singlet), d (doublet), t (triplet), and m (multiplet). FAB-MS and MALDI-TOF-MS spectra were recorded with *m*-nitrobenzyl alcohol (NBA) and dithranol (Dith) as a matrix, respectively. The most important signals are reported in *m*/*z* units with M as the molecular ion. Electronic absorption spectra were measured in a cuvette of 1 cm at room temperature. The absorption maxima (λ_{max}) are reported in nm with the relative intensity or the molar absorptivity in brackets. Recycling gel-permeation chromatography (GPC) eluting $CHCl_3$ was performed with UV detectors using 1H and 2H polystyrene columns. Cyclic voltammetry and differential pulse voltammetry were performed by using a cell equipped with a platinum as working electrode, a platinum wire as counter electrodes, and $Ag/AgNO_3$ as the referential electrode. All electrochemical measurements were performed in *o*-DCB solution (*ca.* 5×10^{-4} mol L^{-1}) containing 0.1 mol L^{-1} *n*-Bu_4NPF_6 at room temperature. All potentials are referenced to the ferrocenium/ferrocene (Fc^+/Fc) couple, used as a standard. PXRD measurements for the materials from **1** and **3** through a phase transfer method were performed on an X-ray diffractometer for which a Cu–Kα radiation (λ = 1.54 Å) was used.

2. Synthesis

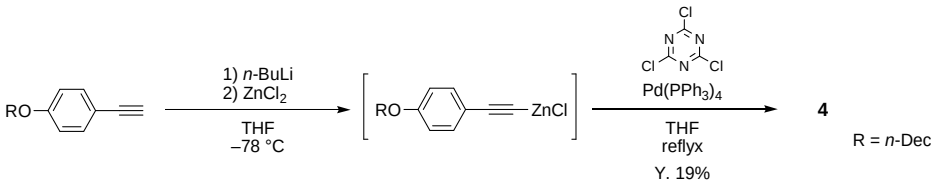

Scheme S1. Synthesis of reference compound **4**.

***Preparation of 2-[4-(Decyloxy)phenyl]-1,3-thiazole* (10).** A solution of **9** (198 mg, 0.549 mmol) and $NaHCO_3$ (95 mg, 1.1 mmol) in a mixture of DME/water (4:1, 25 mL) was bubbled with argon for 0.5 h. $Pd(PPh_3)_4$ (26 mg, 0.02 mmol) and 2-bromothiazole (148 mg, 0.902 mmol) were added to the mixture. The resulting mixture was refluxed for 6.5 h. After addition of water (50 mL), the organic phase was separated and the aqueous phase was extracted with toluene/ethyl acetate (1:1, 50 mL × 3). The combined organic phase was dried over anhydrous $MgSO_4$ and concentrated under reduced pressure. The residue was purified by column chromatography (SiO_2, toluene/hexane 4:1) to give **10** (124 mg, 0.391 mmol, 71%) as white solids. M.p. 63–64 °C; ^{1}H NMR (400 MHz, $CDCl_3$): δ 7.89 (2H, d, J = 8.8 Hz), 7.80 (1H, d, J = 3.3 Hz), 7.24 (1H, d, J = 3.3 Hz), 6.94 (2H, d, J = 8.8 Hz), 4.00 (2H, t, J = 6.6 Hz), 1.80 (2H, dt, J = 6.6, 7.5 Hz), 1.50–1.28 (14H, m), 0.89 (3H, t, J = 7.0 Hz); ^{13}C NMR (75 MHz, $CDCl_3$): δ 168.5, 160.8, 143.4, 128.1, 126.4, 117.8, 114.9, 68.2, 32.0, 29.7, 29.53, 29.47, 29.3, 26.1, 22.8, 14.2 (1 signal was missing); UV–vis ($CHCl_3$): λ_{max} (ε) 302 nm (19000 L mol^{-1} cm^{-1}); MALDI-TOF-MS (Dith, positive) m/z 318 [$(M + H)^+$]; elemental analysis: calcd (%) $C_{19}H_{27}NOS$: C 71.88, H 8.57, N 4.41, found: C 71.64, H 8.38, N 4.41.

***Preparation of 5-Bromo-2-[4-(decyloxy)phenyl]-1,3-thiazole* (11).** To a solution of **10** (458 mg, 1.44 mmol) in 1,2-dichloroethane (15 mL) was added *N*-bromosuccinimide (261 mg, 1.46 mmol) at room temperature. The resulting mixture was refluxed for 19 h. After addition of water (50 mL), the organic phase was separated and the aqueous phase was extracted with $CHCl_3$ (50 mL × 3). The resulting solution was dried over anhydrous $MgSO_4$ and concentrated under reduced pressure. The residue was purified by column chromatography (SiO_2, toluene/hexane 4:1) to give **11** (537 mg, 1.35 mmol, 94%) as white solids. M.p. 69–70 °C; ^{1}H NMR (400 MHz, $CDCl_3$): δ 7.78 (2H, d, J = 8.9 Hz), 7.66 (1H, s), 6.93 (2H, d, J = 8.9 Hz), 4.00 (2H, t, J = 6.6 Hz), 1.80 (2H, dt, J = 6.6, 7.5 Hz), 1.46 (2H, dt, J = 7.1, 7.5 Hz), 1.43–1.27 (12H, m), 0.89 (3H, t, J = 7.0 Hz); ^{13}C NMR ($CDCl_3$, 75 MHz): δ 169.6, 161.1, 144.6, 127.7, 125.9, 114.9, 107.2, 68.3, 32.0, 29.7, 29.52, 29.46, 29.3, 26.1, 22.8, 14.2 (1 signal was missing); UV–vis (CH_2Cl_2): λ_{max} (ε) 314 nm (20300 L mol^{-1} cm^{-1}); MALDI-TOF-MS (Dith, positive): m/z 397 (M^+); elemental analysis: calcd (%) $C_{19}H_{26}BrNOS$: C 57.57, H 6.61, N 3.53, found: C 57.51, H 6.58, N 3.53.

***Preparation of 2-[4-(Decyloxy)phenyl]-5-(tributyltin)-1,3-thiazole* (6).** To a solution of **11** (499 mg, 1.13 mmol) in THF (15 mL) was added dropwise a *n*-BuLi hexane solution (1.60 mol L^{-1}, 0.95 mL, 1.52 mmol) at −78 °C under argon atmosphere. After the mixture was stirred at −78 °C for 1 h,

tributyltin chloride (600 mg, 1.84 mmol) was added to the mixture at −78 °C. The resulting mixture was stirred at room temperature for 1 h. After addition of water (50 mL), the organic phase was separated and the aqueous phase was extracted with ethyl acetate (50 mL × 3). The combined organic phase was dried over sodium sulfate and concentrated under reduced pressure. The residue was purified by column chromatography (Al_2O_3, toluene) to give **6** (652 mg, 1.07 mmol, 95%) as yellow oil. ^{1}H NMR (400 MHz, $CDCl_3$): δ 7.91 (2H, d, J = 8.9 Hz), 7.73 (1H, s), 6.94 (2H, d, J = 8.9 Hz), 3.99 (2H, t, J = 6.6 Hz), 1.80 (2H, dt, J = 6.6, 7.5 Hz), 1.68–1.52 (6H, m), 1.47 (2H, dt, J = 6.8, 7.4 Hz), 1.40–1.28 (18H, m), 1.24–1.07 (6H, m), 0.93–0.87 (12H, m); ^{13}C NMR (75 MHz, $CDCl_3$): δ 173.3, 160.5, 150.0, 128.1, 127.4, 126.7, 114.8, 68.2, 32.0, 29.7, 29.56, 29.48, 29.38, 29.0, 27.3, 26.1, 22.8, 14.2, 13.8, 11.1 (1 signal was missing); UV–vis ($CHCl_3$): λ_{max} (ε) 309 nm (26500 L mol^{-1} cm^{-1}); MALDI-TOF-MS (Dith, positive): m/z 608 [(M + H)$^+$]; elemental analysis: calcd (%) $C_{31}H_{53}NOSSn$: C 61.39, H 8.81, N 2.31, found: C 61.33, H 8.84, N 2.26.

***Preparation of Tris({2-[4-(decyloxy)phenyl]-1,3-thiazol-5-yl})-1,3,5-triazine* (1).** A solution of **6** (652 mg, 1.07 mmol) in 1,4-dioxane (20 mL) was bubbled with argon for 0.5 h. $Pd_2(dba)_3\cdot CHCl_3$ (26 mg, 0.03 mmol), tributylphosphonium tetrafluoroborate (44 mg, 0.15 mmol), CsF (92 mg, 0.61 mmol), and 2,4,6-trichloro-1,3,5-triazine (**5**) (45 mg, 0.24 mmol) were added to the mixture at room temperature. The resulting mixture was stirred at 40 °C for 24 h. After addition of water (100 mL), the organic phase was separated and the aqueous phase was extracted with ethyl acetate (100 mL × 3). The combined organic phase was dried over anhydrous Na_2SO_4 and concentrated under reduced pressure. The residue was purified by column chromatography (SiO_2, $CHCl_3$) to give **1** (136 mg, 0.132 mmol, 54%) as yellow solids. M.p. 139–140 °C; ^{1}H NMR (600 MHz, $CDCl_3$): δ 8.85 (3H, s), 8.03 (6H, d, J = 8.8 Hz), 6.99 (6H, d, J = 8.8 Hz), 4.04 (6H, t, J = 6.6 Hz), 1.83 (6H, dt, J = 6.6, 7.2 Hz), 1.49 (6H, dt, J = 7.2, 7.8 Hz), 1.39–1.26 (36H, m), 0.89 (9H, t, J = 6.9 Hz); ^{13}C NMR (75 MHz, $CDCl_3$): δ 173.1, 166.4, 161.4, 147.9, 134.9, 128.3, 125.8, 114.6, 68.2, 32.0, 29.8, 29.6, 29.5, 29.4, 26.2, 22.8, 14.3 (1 signal was missing); UV–vis ($CHCl_3$): λ_{max} (ε) 381 (77000), 385 nm (75700 L mol^{-1} cm^{-1}); HR-FAB-MS (NBA, positive): m/z calcd for $C_{60}H_{79}N_6O_3S_3^+$ 1027.5376, found 1027.5375 [(M + H)$^+$].

***Preparation of 4-Bromo-2-[4-(decyloxy)phenyl]-1,3-thiazole* (12).** To a solution of **11** (939 mg, 2.37 mmol) in THF (15 mL) was added dropwise to a freshly prepared LDA THF solution (0.84 mol L^{-1}, 3.7 mL, 3.11 mmol) at −78 °C under argon atmosphere. After the mixture was stirred at −78 °C for 0.5 h, water (1.3 mL) was added at the same temperature and the resulting mixture was allowed to warm to room temperature. After addition of water (100 mL), the organic phase was separated and the aqueous phase was extracted with ethyl acetate (100 mL × 3). The combined organic phase was washed with brine (100 mL), dried over $MgSO_4$, and concentrated under reduced pressure. The residue was purified by column chromatography (SiO_2, toluene) to give **12** (476 mg, 1.20 mmol, 55%) as white solids. M.p. 77–78 °C; 1H NMR (400 MHz, CDCl3): δ 7.86 (2H, d, J = 8.9 Hz), 7.12 (1H, s), 6.93 (2H, d, J = 8.9 Hz), 4.00 (2H, t, J = 6.6 Hz), 1.80 (2H, dt, J = 6.6 Hz, 7.4 Hz), 1.50–1.28 (14H, m), 0.89 (3H, t, J = 6.8 Hz); ^{13}C NMR ($CDCl_3$, 75 MHz): δ 169.0, 161.3, 127.9, 125.7, 125.3, 115.3, 114.8, 68.3, 32.0, 29.6, 29.51, 29.45, 29.2, 26.1, 22.8, 14.2 (1 signal was missing); UV–vis ($CHCl_3$):

λ_{max} (ε) 313 nm (25400 L mol^{-1} cm^{-1}); MALDI-TOF-MS (Dith, positive): *m*/*z* 397 (M^+); elemental analysis: calcd (%) $C_{19}H_{26}BrNOS$: C 57.57, H 6.61, N 3.53, found: C 57.55, H 6.63, N 3.46.

***Preparation of 2-[4-(Decyloxy)phenyl]-4-(tributyltin)-1,3-thiazole* (7).** To a solution of **12** (1.06 g, 2.68 mmol) in Et_2O (20 mL) was added dropwise a *n*-BuLi hexane solution (2.66 mol L^{-1}, 1.20 mL, 3.19 mmol) at −78 °C under argon atmosphere. After the mixture was warmed to −50 °C and stirred for 0.5 h. The mixture was cooled to −78 °C and tributyltin chloride (1.20 g, 3.68 mmol) was added to the mixture. The mixture was warmed to room temperature and stirred for 1 h. After addition of water (100 mL), the organic phase was separated and the aqueous phase was extracted with ethyl acetate (100 mL × 3). The combined organic phase was washed with brine (100 mL), dried over anhydrous Na_2SO_4, and concentrated under reduced pressure. The residue was purified by column chromatography (Al_2O_3, toluene/hexane 1:4) to give **7** (1.42 g, 2.34 mmol, 87%) as pale yellow oil. ^{1}H NMR (400 MHz, $CDCl_3$): δ 7.91 (2H, d, *J* = 8.9 Hz), 7.23 (1H, s), 6.93 (2H, d, *J* = 8.9 Hz), 4.00 (2H, t, *J* = 6.6 Hz), 1.80 (2H, dt, *J* = 6.6, 7.4 Hz), 1.67–1.52 (6H, m), 1.47 (2H, dt, *J* = 6.6, 7.6 Hz), 1.41–1.28 (18H, m), 1.23–1.05 (6H, m), 0.92–0.87 (12H, m); ^{13}C NMR ($CDCl_3$, 75 MHz): δ 168.2, 160.6, 160.4, 128.5, 127.1, 124.5, 114.7, 68.2, 32.0, 29.7, 29.57, 29.49, 29.3, 29.2, 29.0, 27.4, 26.1, 22.8, 14.3, 13.9, 10.4; UV–vis ($CHCl_3$): λ_{max} (ε) 303 nm (15100 L mol^{-1} cm^{-1}); MALDI-TOF-MS (Dith, positive): *m*/*z* 607 (M^+); elemental analysis: calcd (%) $C_{31}H_{53}NOSSn$: C 61.39, H 8.81, N 2.31, found: C 61.35, H 8.86, N 2.30.

***Preparation of Tris({2-[4-(decyloxy)phenyl]-1,3-thiazol-4-yl})-1,3,5-triazine* (2).** A solution of **7** (700 mg, 1.15 mmol) in 1,4-dioxane (20 mL) was bubbled with argon for 0.5 h. $Pd_2(dba)_3 \cdot CHCl_3$ (31 mg, 0.03 mmol), tributylphosphonium tetrafluoroborate (50 mg, 0.27 mmol), CsF (91 mg, 0.60 mmol), and 2,4,6-trichloro-1,3,5-triazine (**5**) (50 mg, 0.271 mmol) were added to the mixture at room temperature. The resulting mixture was refluxed for 25 h. After addition of water (100 mL), the organic phase was separated and the aqueous phase was extracted with ethyl acetate (100 mL × 3). The combined organic phase was dried over anhydrous Na_2SO_4 and concentrated under reduced pressure. The residue was purified by column chromatography (Al_2O_3, $CHCl_3$) to give **2** (160 mg, 0.156 mmol, 58%) as yellow solids. M.p. > 200 °C (decomp.); ^{1}H NMR (600 MHz, $CDCl_3$): δ 8.76 (3H, s), 8.09 (6H, d, *J* = 8.8 Hz), 7.02 (6H, d, *J* = 8.8 Hz), 4.04 (6H, t, *J* = 6.6 Hz), 1.83 (6H, dt, *J* = 6.6, 7.5 Hz), 1.51–1.25 (42H, m), 0.89 (9H, t, *J* = 7.0 Hz); ^{13}C NMR (75 MHz, $CDCl_3$): δ 169.8, 167.8, 161.3, 153.3, 128.7, 126.2, 125.7, 115.0, 68.3, 32.0, 29.7, 29.56, 29.49, 29.3, 26.1, 22.8, 14.2 (1 signal was missing); UV–vis ($CHCl_3$): λ_{max} (ε) 310 nm (62600 L mol^{-1} cm^{-1}); HR-FAB-MS (NBA, positive): *m/z* calcd for $C_{60}H_{79}N_6O_3S_3^+$ 1027.5376, found 1027.5376 [$(M + H)^+$].

***Preparation of 2-{2-[4-(Decyloxy)phenyl]ethynyl}-1,3-thiazole* (13).** A solution of 1-(decyloxy)-4-ethynylbenzene (807 mg, 3.12 mmol) and aqueous 2-ethanolamine (0.5 mol L^{-1}, 11.2 mL, 5.60 mmol) in THF (20 mL) was bubbled with argon for 0.5 h. $Pd(PPh_3)_2Cl_2$ (63 mg, 0.09 mmol), CuI (11 mg, 0.06 mmol), and 2-bromothiazole (463 mg, 2.82 mmol) were added to the mixture at room temperature. The resulting mixture was stirred at 60 °C for 6.5 h. After addition of water (100 mL), the organic phase was separated and the aqueous phase was extracted with $CHCl_3$ (100 mL × 3). The combined organic phase was washed with water (100 mL), dried over anhydrous $MgSO_4$, and concentrated under reduced pressure. The residue was purified by column chromatography (SiO_2, toluene/hexane 4:1) to give **13** (609 mg, 1.78 mmol, 63%) as white solids. M.p. 62–64 °C; ^{1}H NMR (400 MHz, $CDCl_3$): δ 7.83 (1H, d, J = 3.6 Hz), 7.52 (2H, d, J = 8.8 Hz), 7.34 (1H, d, J = 3.6 Hz), 6.88 (2H, d, J = 8.8 Hz), 3.98 (2H, t, J = 6.6 Hz), 1.79 (2H, dt, J = 6.6, 7.4 Hz), 1.45–1.28 (14H, m), 0.89 (3H, t, J = 6.8 Hz); ^{13}C NMR (75 MHz, $CDCl_3$): δ 160.2, 149.3, 143.5, 133.6, 120.3, 114.7, 113.1, 94.5, 81.3, 68.2, 32.0, 29.6, 29.48, 29.43, 29.2, 26.1, 22.8, 14.2 (1 signal was missing); UV–vis ($CHCl_3$): λ_{max} (ε) 317 nm (24200 L mol^{-1} cm^{-1}); MALDI-TOF-MS (Dith, positive): m/z 341 (M^+); elemental analysis: calcd (%) $C_{21}H_{27}NOS$: C 73.86, H 7.97, N 4.10, found: C 73.62, H 7.93, N 4.04.

***Preparation of 2-{2-[4-(Decyloxy)phenyl]ethynyl}-5-(tributyltin)-1,3-thiazole* (8).** To a solution of **13** (1.00 g, 2.93 mmol) in THF (20 mL) was added dropwise a freshly prepared LDA THF solution (0.83 mol L^{-1}, 3.7 mL, 3.07 mmol) at −78 °C under argon atmosphere. The resulting mixture was warmed to 0 °C and stirred for 1 h. The mixture was cooled to −78 °C and tributyltin chloride (1.80 g, 5.52 mmol) was added to the mixture. The resulting mixture was warmed to 0 °C and stirred for 3 h. After addition of water (100 mL), the organic phase was separated and the aqueous phase was extracted with ethyl acetate (100 mL × 3). The combined organic phase was dried over anhydrous Na_2SO_4 and concentrated under reduced pressure. The residue was purified by column chromatography (Al_2O_3, hexane to toluene) to give **8** (1.42 g, 2.25 mmol, 77%) as yellow oil. ^{1}H NMR ($CDCl_3$, 400 MHz): δ 7.76 (1H, s), 7.51 (2H, d, J = 8.9 Hz), 6.87 (2H, d, J = 8.9 Hz), 3.97 (2H, t, J = 6.6 Hz), 1.79 (2H, dt, J = 6.6, 7.4 Hz), 1.63–1.52 (6H, m), 1.45 (2H, dt, J = 6.7, 7.6 Hz), 1.39–1.28 (18H, m), 1.24–1.07 (6H, m), 0.92–0.87 (12H, m); ^{13}C NMR (75 MHz, $CDCl_3$): δ 160.0, 154.0, 149.8, 133.4, 131.3, 114.7, 113.6, 95.5, 81.5, 68.2, 32.0, 29.6, 29.49, 29.44, 29.2, 29.0, 27.3, 26.1, 22.8, 14.2, 13.7, 11.2 (1 signal was missing); UV–vis ($CHCl_3$): λ_{max} (ε) 323 nm (26300 L mol^{-1} cm^{-1}); MALDI-TOF-MS (Dith, positive): m/z 631 (M^+); elemental analysis: calcd (%) $C_{33}H_{53}NOSSn$: C 62.86, H 8.47, N 2.22, found: C 62.73, H 8.54, N 2.26.

***Preparation of Tris(2-{2-[4-(decyloxy)phenyl]ethynyl}-1,3-thiazol-5-yl)-1,3,5-triazine* (3).** A solution of **8** (1.84 g, 2.94 mmol) in toluene (35 mL) was bubbled with argon for 0.5 h. $Pd_2(dba)_3 \cdot CHCl_3$ (66 mg, 0.06 mmol), triphenylarsine (90 mg, 0.29 mmol), and 2,4,6-trichloro-1,3,5-triazine (**5**) (120 mg, 0.651 mmol) were added to the mixture at room temperature and the resulting mixture was refluxed for 51 h. After addition of water (100 mL), the organic phase was separated and the aqueous phase was extracted with ethyl acetate (100 mL × 3). The combined organic phase was dried over anhydrous $MgSO_4$ and concentrated under reduced pressure. The residue was purified by column chromatography (SiO_2, hexane/$CHCl_3$ 1:4) and washed with acetone to give **3** (103 mg, 0.146 mmol, 14%) as yellow solids. M.p. 177–179 °C; ^{1}H NMR ($CDCl_3$, 400 MHz): δ 8.84 (3H,

s), 8.02 (6H, d, J = 8.8 Hz), 6.99 (6H, d, J = 8.8 Hz), 4.04 (6H, t, J = 6.6 Hz), 1.83 (6H, dt, J = 6.6, 7.5 Hz), 1.49 (6H, dt, J = 6.8, 7.5 Hz), 1.45–1.25 (36H, m), 0.89 (9H, t, J = 6.8 Hz); ^{13}C NMR (75 MHz, $CDCl_3$): δ 166.6, 160.7, 154.5, 148.1, 136.6, 134.0, 114.8, 112.6, 98.2, 82.1, 68.3, 32.0, 29.8, 29.7, 29.54, 29.47, 29.2, 26.1, 22.8, 14.2; UV–vis ($CHCl_3$): λ_{max} (ε) 393 (83400), 400 nm (83100 L mol^{-1} cm^{-1}); HR-FAB-MS (NBA, positive): m/z calcd for $C_{66}H_{79}N_6O_3S_3^+$ 1099.5376, found 1099.5378 [(M + H)$^+$].

***Preparation of Tris({2-[4-(decyloxy)phenyl]ethynyl})-1,3,5-triazine* (4).** To a solution of 1-(decyloxy)-4-ethynylbenzene (370 mg, 1.43 mmol) in THF (6 mL) was added dropwise a *n*-BuLi hexane solution (1.60 mol L^{-1}, 1.3 mL, 2.08 mmol) at −78 °C under argon atmosphere. After the mixture was stirred at −78 °C for 1 h, a $ZnCl_2$ THF solution (0.20 mol L^{-1}, 11.7 mL, 2.34 mmol) was added. After the mixture was stirred at −78 °C for 1 h, the resulting mixture was warmed to room temperature. The resulting mixture was stirred for 1 h, a solution of 2,4,6-trichloro-1,3,5-triazine (**5**) (61 mg, 0.33 mmol) and $Pd(PPh_3)_4$ (20 mg, 0.032 mmol) in THF (10 mL) was added dropwise to the mixture at room temperature. After the mixture was refluxed for 18 h, the resulting mixture was filtered through a bed of silica gel (toluene) and the filtered was concentrated under reduced pressure. The residue was purified by column chromatography (SiO_2, hexane/CH_2Cl_2 1:1) to give **4** (53 mg, 0.06 mmol, 19%) as yellow waxy solids. M.p. 40–41 °C; ^{1}H NMR (400 MHz, $CDCl_3$): δ 7.64 (6H, d, J =8.9 Hz), 6.90 (6H, d, J = 8.9 Hz), 4.00 (6H, t, J = 6.6 Hz), 1.80 (6H, dt, J = 6.7, 7.4 Hz), 1.49–1.28 (42H, m), 0.89 (9H, t, J = 6.9 Hz); ^{13}C NMR (75 MHz, $CDCl_3$): δ 161.3, 160.6, 135.2, 114.9, 112.0, 94.9, 86.5, 68.3, 32.0, 29.6, 29.48, 29.46, 29.21, 26.11, 22.8, 14.2 (1 signal was missing); UV–vis ($CHCl_3$): λ_{max} (ε) 362 nm (92600 L mol^{-1} cm^{-1}); MALDI-TOF-MS (Dith, positive): m/z 850 [(M + H)$^+$]; HR-FAB-MS (NBA, positive): m/z calcd for $C_{57}H_{76}N_3O_3^+$ 850.5887, found 850.5886 [(M + H)$^+$].

3. Photophysical properties

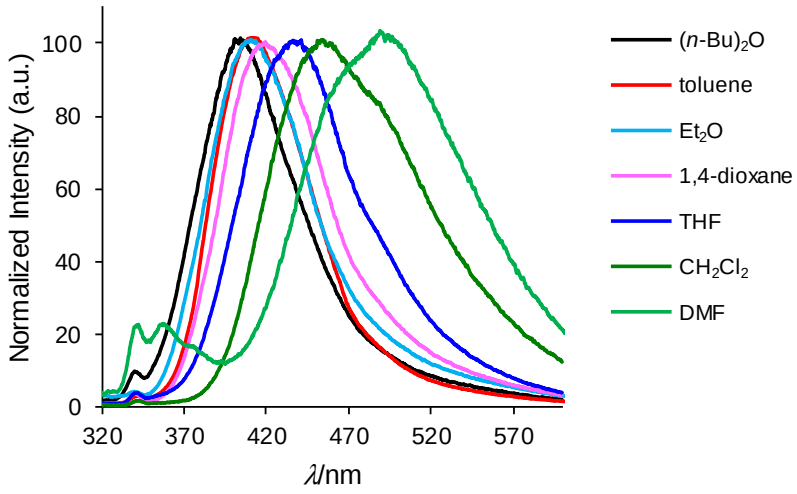

Figure S1. Fluorescence spectra of **2** in $(n\text{-Bu})_2O$, toluene, Et_2O, 1,4-dioxane, THF, CH_2Cl_2, and DMF at RT.

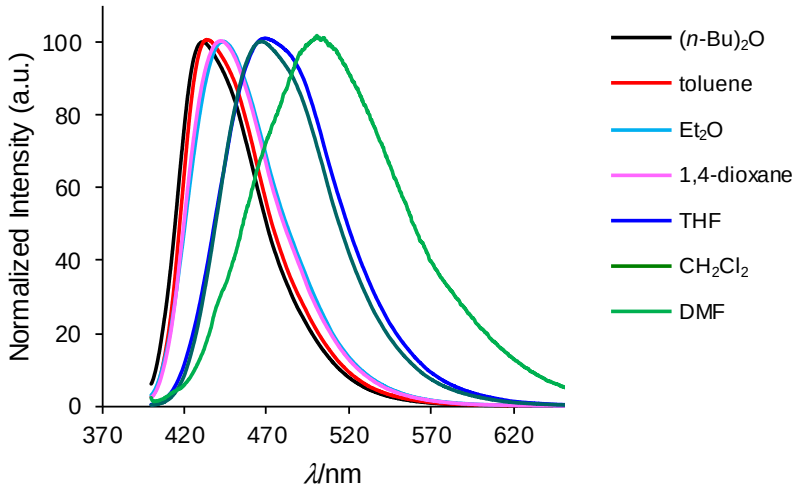

Figure S2. Fluorescence spectra of **3** in $(n\text{-Bu})_2O$, toluene, Et_2O, 1,4-dioxane, THF, CH_2Cl_2, and DMF at RT.

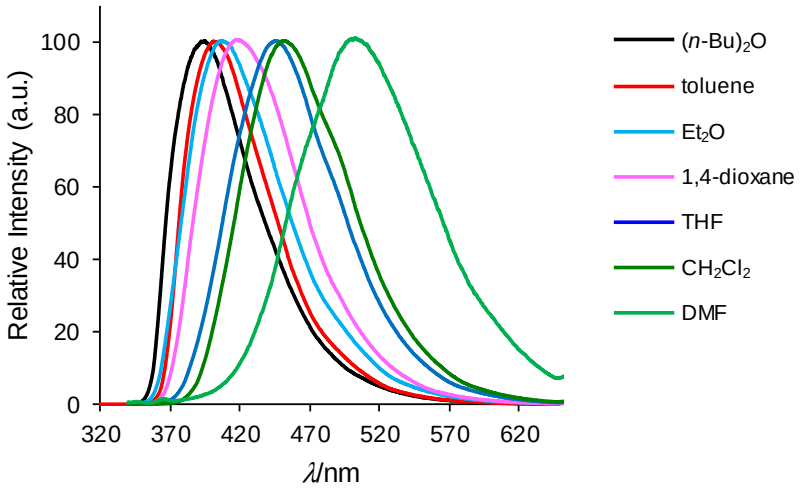

Figure S3. Fluorescence spectra of **4** in $(n\text{-Bu})_2O$, toluene, Et_2O, 1,4-dioxane, THF, CH_2Cl_2, and DMF at RT.

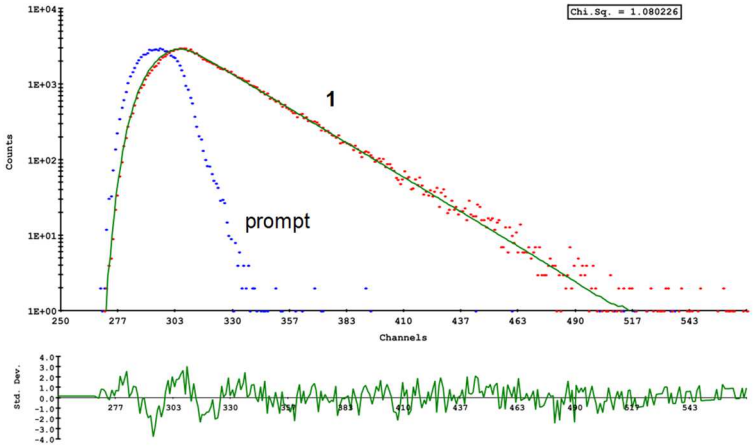

Figure S4. Fluorescence decay curve (top) and residual (bottom) of **1** in CH_2Cl_2.

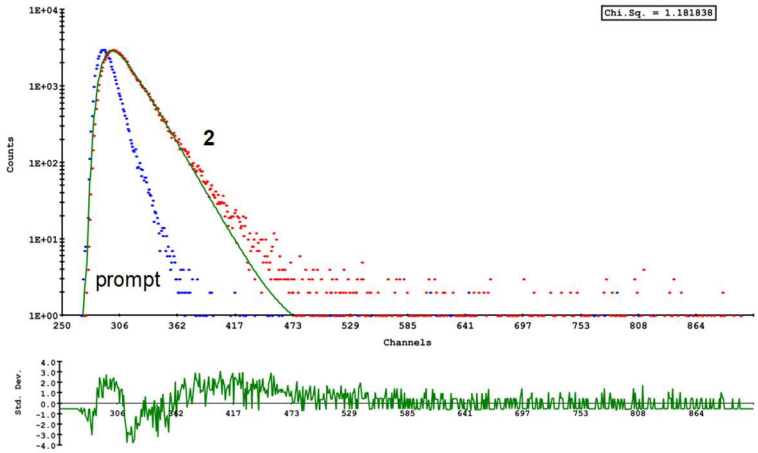

Figure S5. Fluorescence decay curve (top) and residual (bottom) of **2** in CH_2Cl_2.

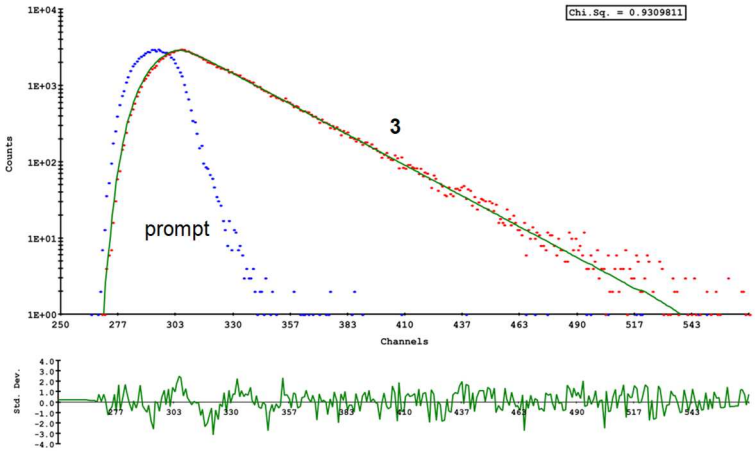

Figure S6. Fluorescence decay curve (top) and residual (bottom) of **3** in CH_2Cl_2.

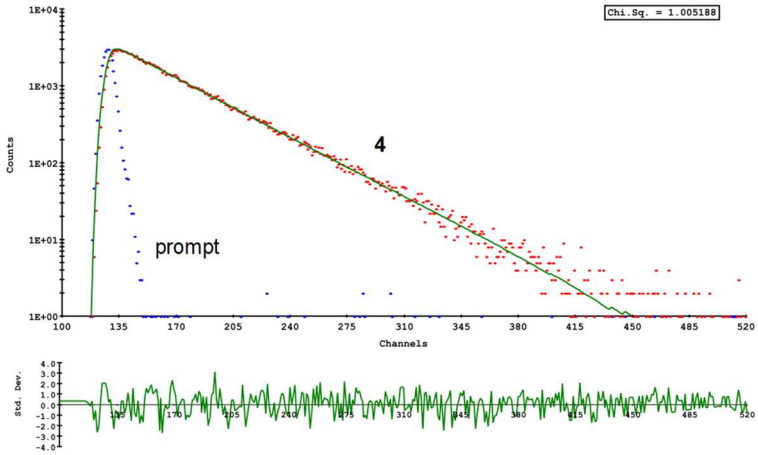

Figure S7. Fluorescence decay curve (top) and residual (bottom) of **4** in CH_2Cl_2.

4. Electrochemical properties

Table S1. Cyclic Voltammetry (CV) and Differential Pulse Voltammetry (DPV) Data of **1**–**4** in *o*-DCB (0.1 mol L^{-1} *n*-Bu_4NPF_6), Theoretically Calculated HOMO–LUMO Gaps (ΔE_{calcd}), Electrochemical Gaps (ΔE_{redox}, $\Delta E°_{redox}$), and Optical Energy Gaps (ΔE_{opt})

	CV [a]		DPV [b]		$\Delta E°_{redox}$/V [a,c]	ΔE_{opt}/eV [e]
	E_{pa}/V	E_{pc}/V	E_{ox}/V	E_{red}/V	(ΔE_{redox}/V [b,d])	(ΔE_{calcd}/eV [f])
1	1.38	−2.22	1.14	−2.01	3.60	3.17
			1.23	−2.53	(3.15)	(3.46)
2	1.45	−2.47	1.11	−2.31	3.92	4.00
			1.18		(3.42)	(3.92)
3	1.30	−1.92	1.17	−1.79	3.22	3.08
		−2.51	1.45	−2.33	(2.96)	(3.21)
4	1.46	−2.18	1.31	−2.03	3.64	3.42
			1.53	−2.11	(3.34)	(3.92)

[a] Scan rate 100 mV s^{-1}. Irreversible wave. [b] Pulse width of 0.1 s in a period of 0.2 s. [c] $\Delta E_{redox} = E_{pa} - E_{pc}$. [d] $\Delta E°_{redox} = E_{ox} - E_{red}$. [e] Optical gap, ΔE_{opt}, is defined as the energy corresponding to the longest λ_{max} in $CHCl_3$. [f] B3LYP/6-31+G(d)//B3LYP/6-31G(d).

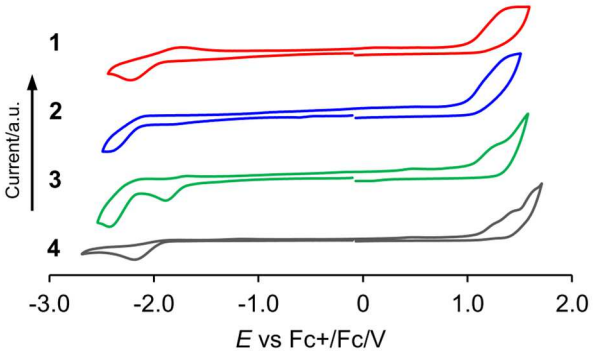

Figure S8. Cyclic voltammograms of **1**–**4** measured in *o*-DCB (0.1 mol L^{-1} *n*-Bu_4NPF_6) at a scan rate of 100 mV s^{-1}.

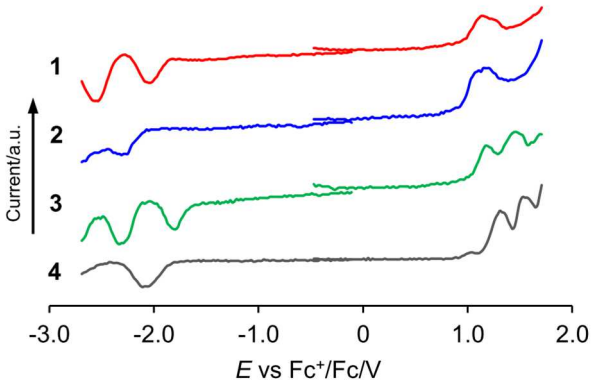

Figure S9. Differential pulse voltammograms of **1**–**4** measured in *o*-DCB (0.1 mol L^{-1} *n*-Bu_4NPF_6) at a pulse width of 0.1 s over a period of 0.2 s.

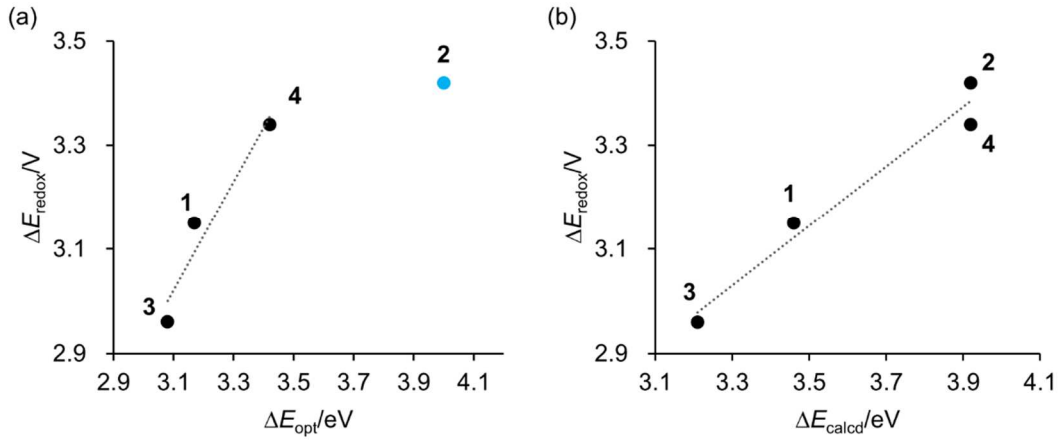

Figure S10. Plots of the ΔE_{redox} values as a function of the (a) ΔE_{opt} and (b) ΔE_{calcd} values for **1**–**4**.

5. Quantum chemical calculations

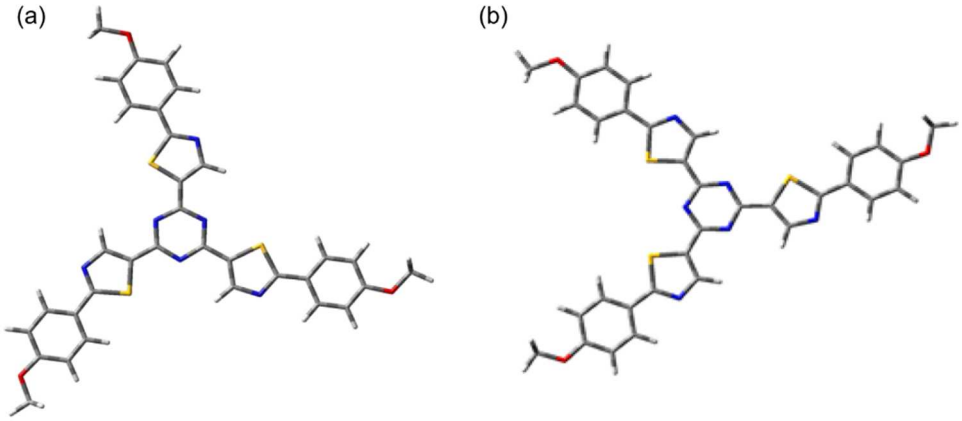

Figure S11. Optimized structures of **1**'with (a) C_{3h} and (b) C_s symmetry at the B3LYP/6-31G(d) level.

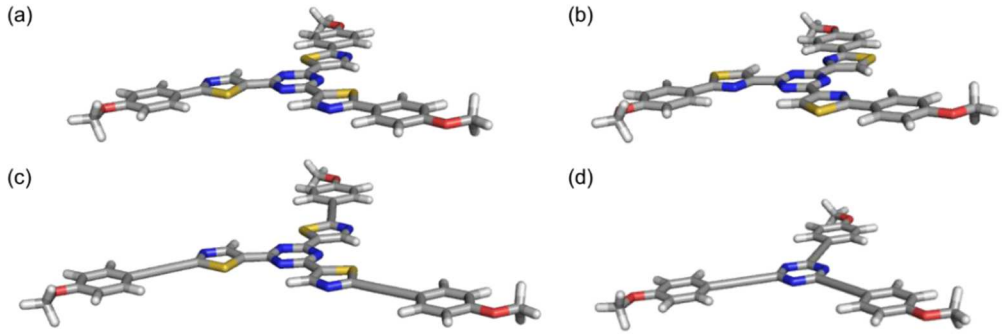

Figure S12. Optimized structures of (a) **1**', (b) **2**', (c) **3**', and (d) **4**' at the B3LYP/6-31G(d) level.

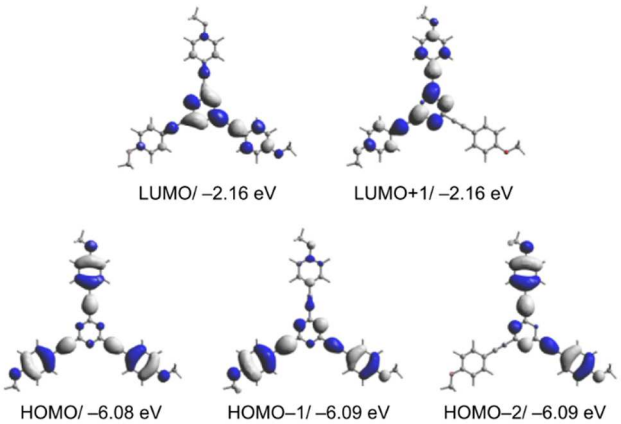

Figure S13. Selected frontier molecular orbitals of **4** at the B3LYP/6-31+G(d,p)//B3LYP/6-31G(d).

Table S2. Summary of TD-DFT Calculations (B3LYP/6-31G(d)) and Assignment of Electronic Absorption in the Longer Wavelength Region for **1**'

λ_{max}^{abs}/nm[a]	λ_{max}^{calcd}/nm	Osc.	Transitions[b]
391	400	0.8033	H–2 → L+1, 3%; H–1 → L, 3%; H → L, 25%; H → L+1, 68%
	400	0.8033	H–2 → L, 3%; H–1 → L+1, 3%; H → L, 68%; H → L+1, 25%
	395	0.3750	H–2 → L, 44%; H–2 → L+1, 2%; H–1 → L, 2%; H–1 → L+1, 44%; H → L, 6%
	395	0.3750	H–2 → L, 2%; H–2 → L+1, 44%; H–1 → L, 44%; H–1 → L+1, 2%; H → L+1, 6%

[a] In $CHCl_3$. [b] H = HOMO; L = LUMO.

Table S3. Summary of TD-DFT Calculations (B3LYP/6-31G(d)) and Assignment of Electronic Absorption in the Longer Wavelength Region for **2**'

λ_{max}^{abs}/nm	λ_{max}^{calcd}/nm	Osc.	Transitions
310	349	0.0558	H–2 → L, 15%; H–2 → L+1, 5%; H–1 → L, 5%; H–1 → L+1, 15%; H → L → 23%, H → L+1, 36%
	349	0.0558	H–2 → L, 15%; H–2 → L+1, 5%; H–1 → L, 5%; H–1 → L+1, 15%; H → L → 23%, H → L+1, 36%
	343	0.1522	H–2 → L, 8%; H–2 → L+1, 20%; H–1 → L, 20%; H–1 → L+1, 8%; H → L, 31%, H → L+1, 6%
	343	0.1522	H–2 → L, 20%; H–2 → L+1, 8%; H–1 → L, 8%; H–1 → L+1, 20%; H → L, 6%, H → L+1, 30%
	306	0.6057	H–2 → L+2, 77%; H–1 → L+2, 11%; H → L+3, 3%
	306	0.6057	H–2 → L+2, 11%; H–1 → L+2, 77%; H → L+3, 3%
	299	0.4825	H–2 → L+2, 8%; H–2 → L+3, 7%; H–2 → L+4, 14%; H–1 → L+3, 14%; H–1 → L+4 → 7%, H → L+3, 35%; H → L+4, 9%
	299	0.4825	H–2 → L+3, 14%; H–2 → L+4, 7%; H–1 → L+2, 8%; H–1 → L+3, 7%; H–1 → L+4 → 14%, H → L+3, 9%; H → L+4, 35%

[a] In $CHCl_3$. [b] H = HOMO; L = LUMO.

Table S4. Summary of TD-DFT Calculations (B3LYP/6-31G(d)) and Assignment of Electronic Absorption in the Longer Wavelength Region for **3'**

λ_{max}^{abs}/nm[a]	λ_{max}^{calcd}/nm	Osc.	Transitions[b]
391	431	1.3416	H–2 → L+1, 3%; H–2 → L+1, 5%; H–1 → L, 5%; H–1 → L+1, 3%; H → L, 70%; H → L+1, 12%
	431	1.3416	H–2 → L+1, 5%; H–2 → L+1, 3%; H–1 → L, 3%; H–1 → L+1, 5%; H → L, 12%; H → L+1, 70%
	424	0.2222	H–2 → L+1, 41%; H–1 → L, 41%; H → L, 3%; H → L+1, 14%
	424	0.2222	H–2 → L, 41%; H–1 → L+1, 41%; H → L, 13%; H → L+1, 3%

[a] In $CHCl_3$. [b] H = HOMO; L = LUMO.

Table S5. Summary of TD-DFT Calculations (B3LYP/6-31G(d)) and Assignment of Electronic Absorption in the Longer Wavelength Region for **4'**

λ_{max}^{abs}/nm[a]	λ_{max}^{calcd}/nm	Osc.	Transitions[b]
363	350	1.0315	H–2 → L, 5%; H–1 → L+1, 5%; H → L, 41%; H → L+1, 49%
	350	1.0315	H–2 → L+1, 5%; H–1 → L, 5%; H → L, 49%; H → L+1, 41%
	348	0.3532	H–2 → L+1, 45%; H–1 → L, 45%; H → L, 5%; H → L+1, 5%
	348	0.3532	H–2 → L, 45%; H–1 → L+1, 45%; H → L, 5%; H → L+1, 5%

[a] In $CHCl_3$. [b] H = HOMO; L = LUMO.

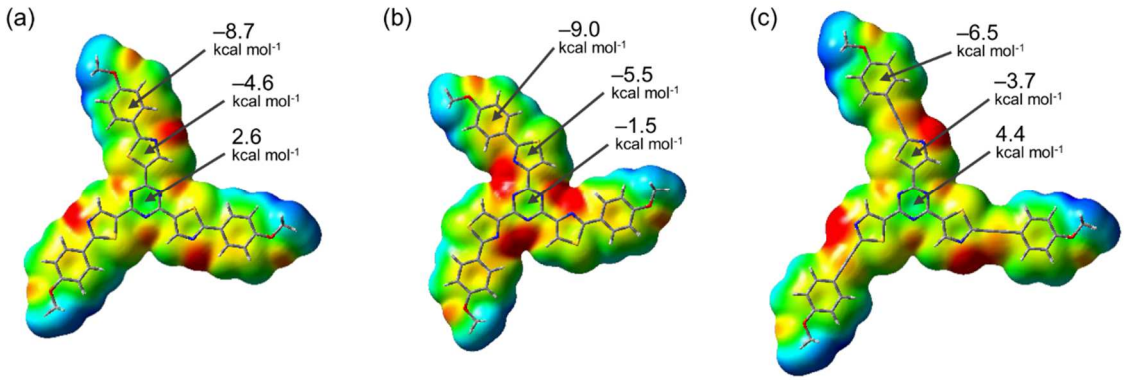

Figure S14. ESPs and values of MEPs; the calculated position of the MEPs are 2Å above the center of the aromatic rings of (a) **1'**, (b) **2'**, and (c) **3'** at the level of B3LYP/6-31+G(d,p)//B3LYP/6-31G(d). The potentials are drawn in the same color scale, with red indicating more-negative potentials and blue, more-positive potentials.

Computational method: We optimized local minima on potential energy surfaces using the B3LYP functional[3,4,5] combined with the 6-31G(d) basis set[6,7] After geometry optimizations, single-point calculations were performed to investigate energies and electronic structures using the 6-31+G(d,p) basis set. To obtain excited states and their oscillator strength TD-DFT[8] calculations were performed at the B3LYP/6-31G(d) level. Self-assembling properties of **1** and **3** were calculated with the counterpoise correction[11] and the empirical dispersion correction at the B97D3/def2-TZVP //B97D3/def2-SVP[9,10] level. The counterpoise correction is a prescription for removing the basis set superposition error. The Gaussian 09 program package[12] was used for all DFT calculations.

ESPs and MEPs estimated by DFT calculations: To gain further insight into the self-association properties of **1**–**3**, we calculated the electrostatic-potential surfaces (ESPs) and molecular electrostatic potentials (MEPs) of **1'**–**3'** at the B3LYP/6-31+G(d,p)//B3LYP/6-31G(d) level (Figure S14). The theoretical results clearly indicate a less-negative character for the aromatic rings of **1** and **3** than **2**, which is consistent with the results of electrochemistry described above; the E_{red} value of **1** and **3** is less negative than that of **2**. According to the well-known polar/π model, the decrease in the electron density of aromatic rings reduces the electrostatic repulsion between π-electrons and strengthen π–π stacking interactions.[13] Hence, the lower electron density of **1** and **3** than **2** is in part responsible for the higher self-association ability of the former than the latter. We note that the aromatic rings of **3** are even less negative than those of **1** as expected from the DPV analyses; the E_{red} value of **3** is less negative than that of **1**. This finding does not account for the lower self-association ability of **3** than **1** in terms of the electron density of the aromatic rings; compound **3** seems to be electronically more favorable than **1** for the self-association.

*Self-assembling properties of **1** and **3**:* We note that the lower K_a value of **3** than **1** cannot be explained from the viewpoint of the extent of the overlap of the aromatic rings in the dimeric structures, which is almost the same in the plausible self-assembled dimers of **1'** and **3'** obtained by DFT calculations. It is known that the rotational barrier for the carbon (sp)–carbon (sp^2) bond is smaller than that for the carbon (sp^2)–carbon (sp^2) bond: for example, the barrier of diphenylethyne is as high as one-third of that of biphenyl.[14] Hence, in the monomeric state the rotation about the acetylenic bonds connecting the thiazole and decyloxybenzene moieties in **3** is assumed to be faster than the rotation about the corresponding single bonds in **1**. Thus, we speculated that the rotation of **3** faster than **1** results in the lower K_a value of **3** than **1**, however, this speculation may conflict the finding that the ΔS value (–24 cal mol^{-1} K^{-1}) for the association of **1** in $CDCl_3$/MCH is more negative than the value (–5.9 cal mol^{-1} K^{-1}) of **3**.

6. Self-association

Table S5. Self-Association Constants (K_a) for **1**–**4** at 20 °C Determined by ^{1}H NMR

	K_a/L mol^{-1}	
	$CDCl_3$	CDC_3/MCH (1:5)
1	8 ± 1	41 ± 2
2	N.D.[a]	N.D.[a]
3	N.D.[a]	20 ± 5
4	N.D.[b]	N.D.[b]

[a] Due to the too small chemical shift change.
[b] Almost no self-association

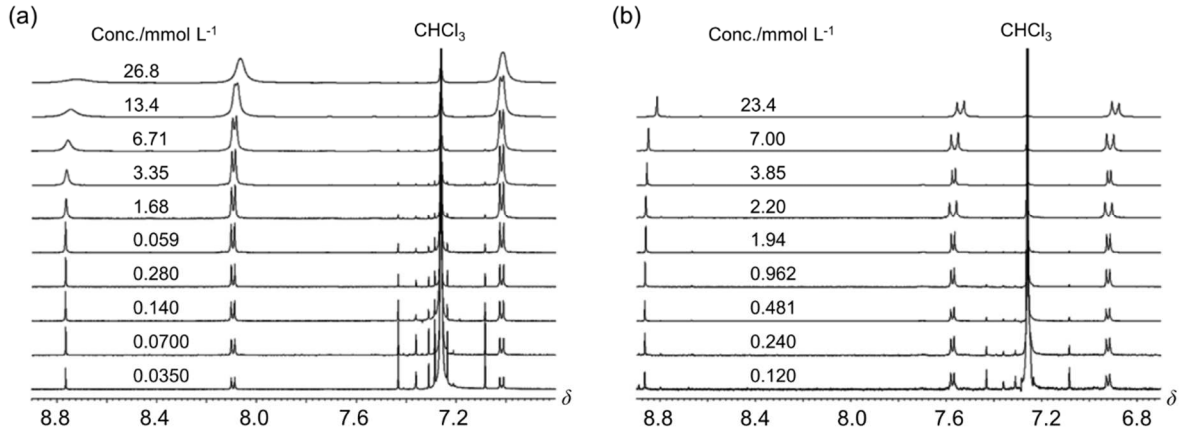

Figure S15. ^{1}H NMR spectra of (a) **2** and (b) **3** in $CDCl_3$ in various concentrations at 20 °C (600 MHz).

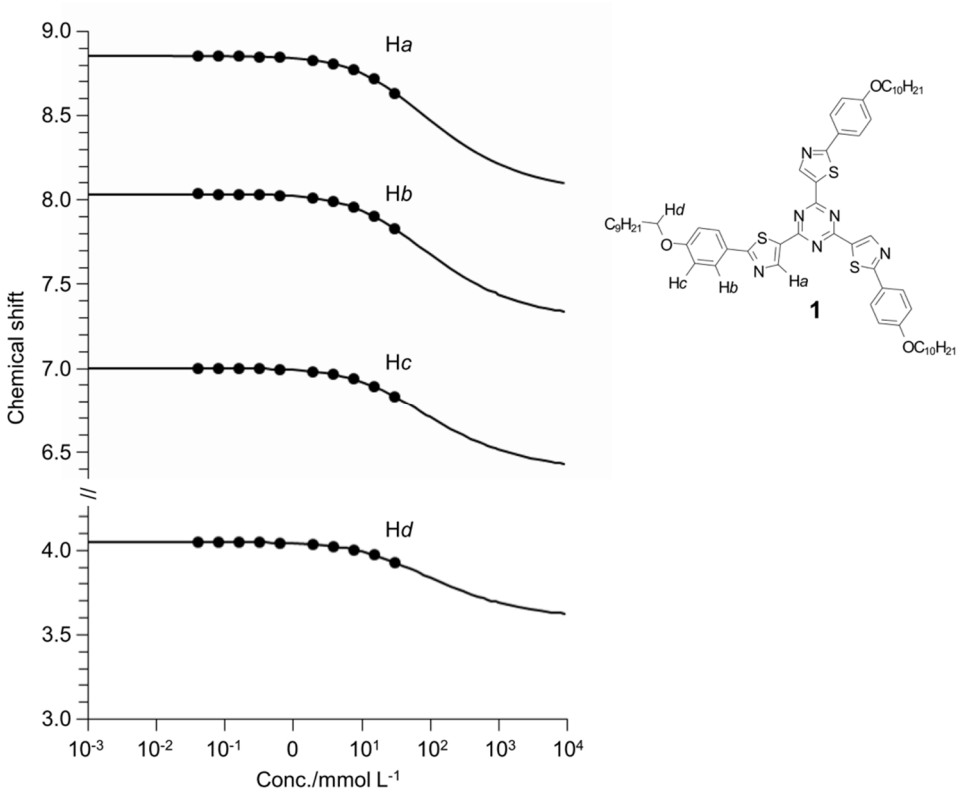

Figure S16. Nonlinear curve-fitting plots of the concentration dependence of the chemical shifts of the aromatic protons of **1** in $CDCl_3$ at 20 °C.

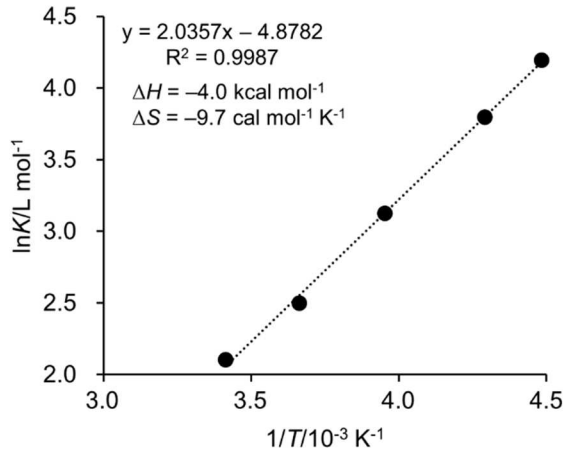

Figure S17. van't Hoff plot for self-association of **1** in $CDCl_3$.

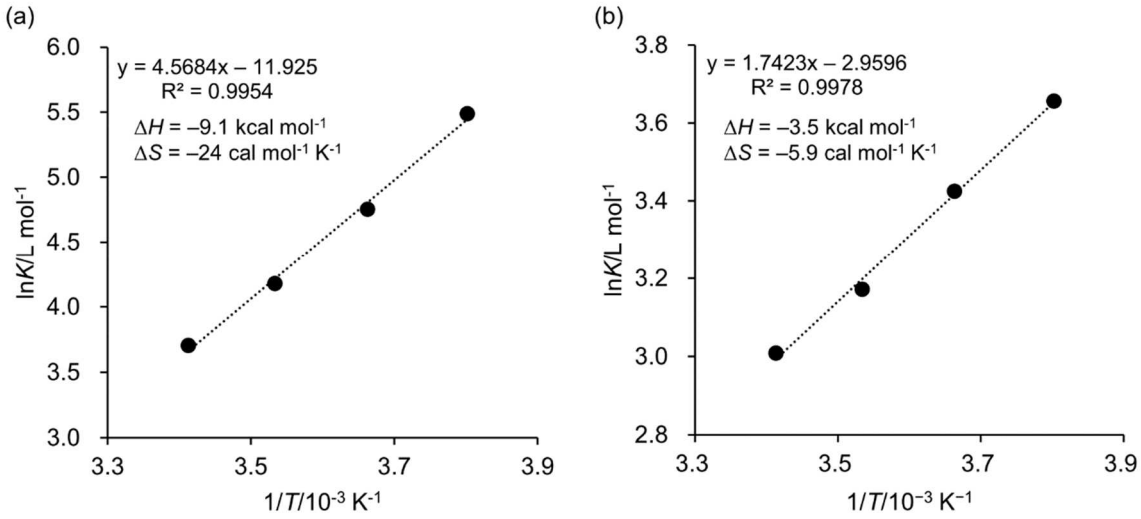

Figure S18. van't Hoff plot for self-association of (a) **1** and (b) **3** in $CDCl_3$/MCH (1:5, v/v).

7. Self-assembly

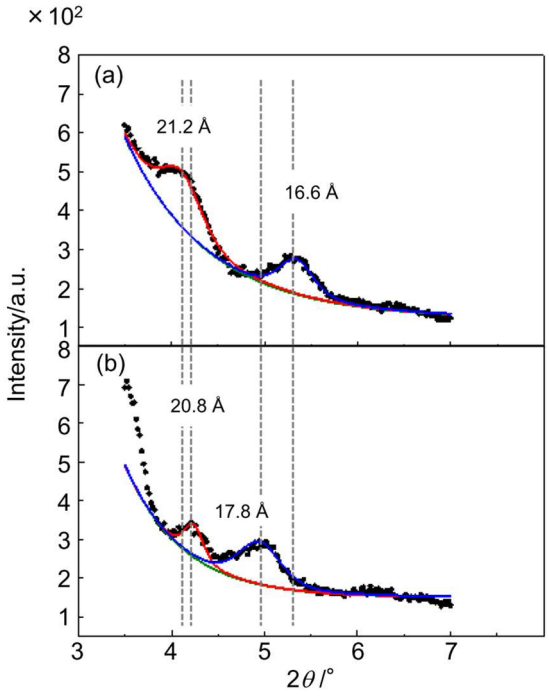

Figure S19. Peak deconvolution analyses of PXRD patterns of precipitates of (a) **1** and (b) **3** obtained from a CH_2Cl_2/MeOH (1:10, v/v) binary solvent system.

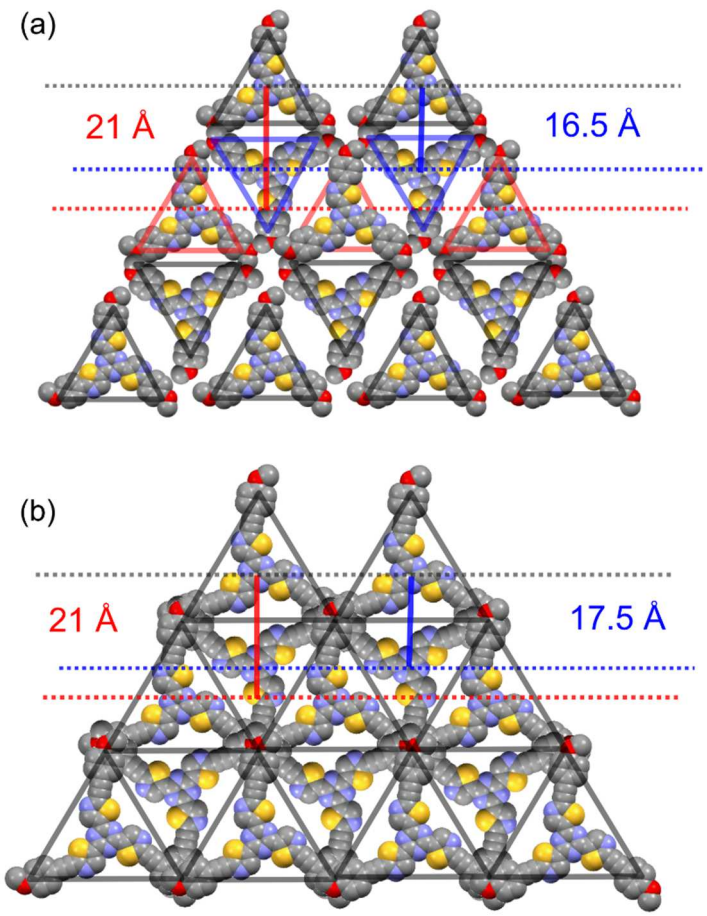

Figure S20. Plausible packing models of the self-assembled clusters of (a) **1** and (b) **3** deduced from PXRD patterns. In these models, decyloxy groups in **1** and **3** were replaced with methyl groups; the monomeric structures were optimized by B3LYP/6-31G(d) level. Hydrogen atoms are omitted for clarity.

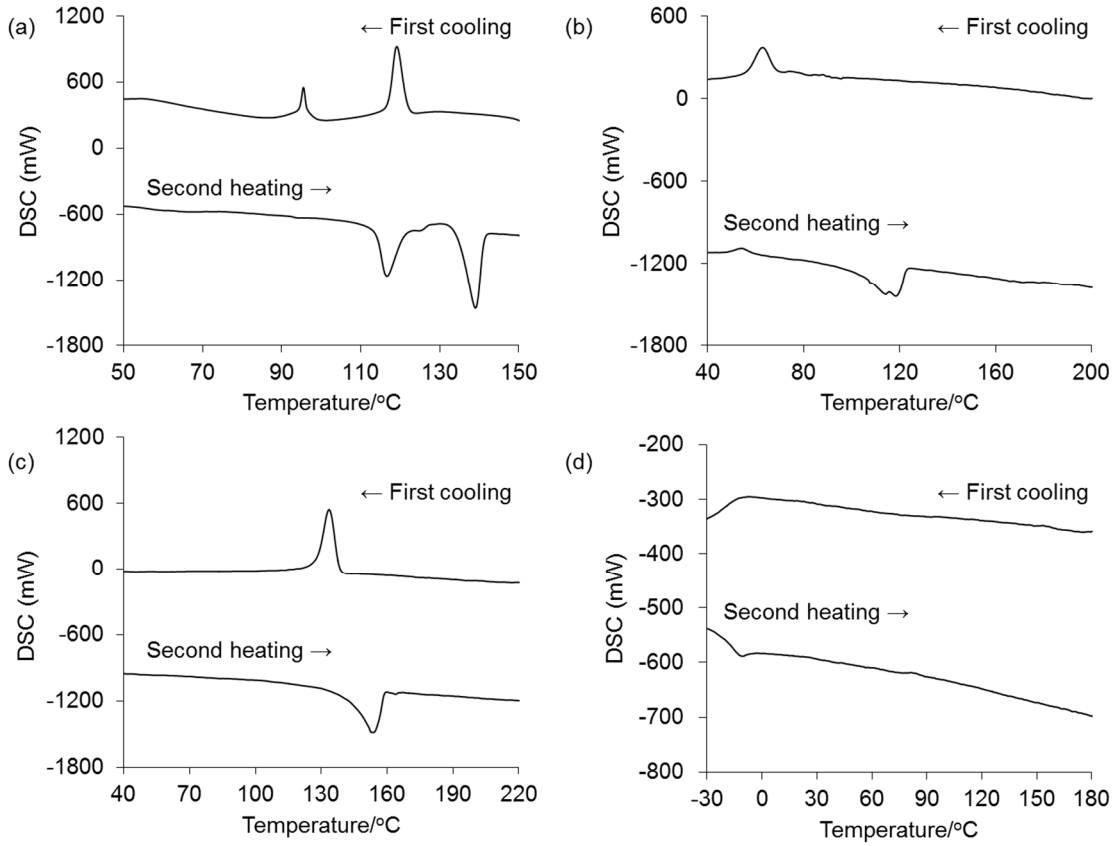

Figure S21. DSC measurement (10 °C min^{-1}) results of (a) **1**, (b) **2**, (c) **3**, and (d) **4**.

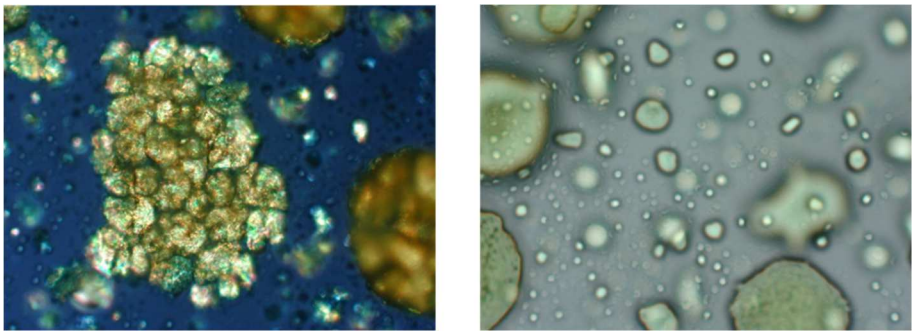

Figure S22. Polarizing microscopic images of **1** at (left) 100 °C and (right) 150 °C. The thermal transition at 96 °C in **1** is attributed to crystal-to-crystal transition.

8. ^{1}H and ^{13}C NMR spectra

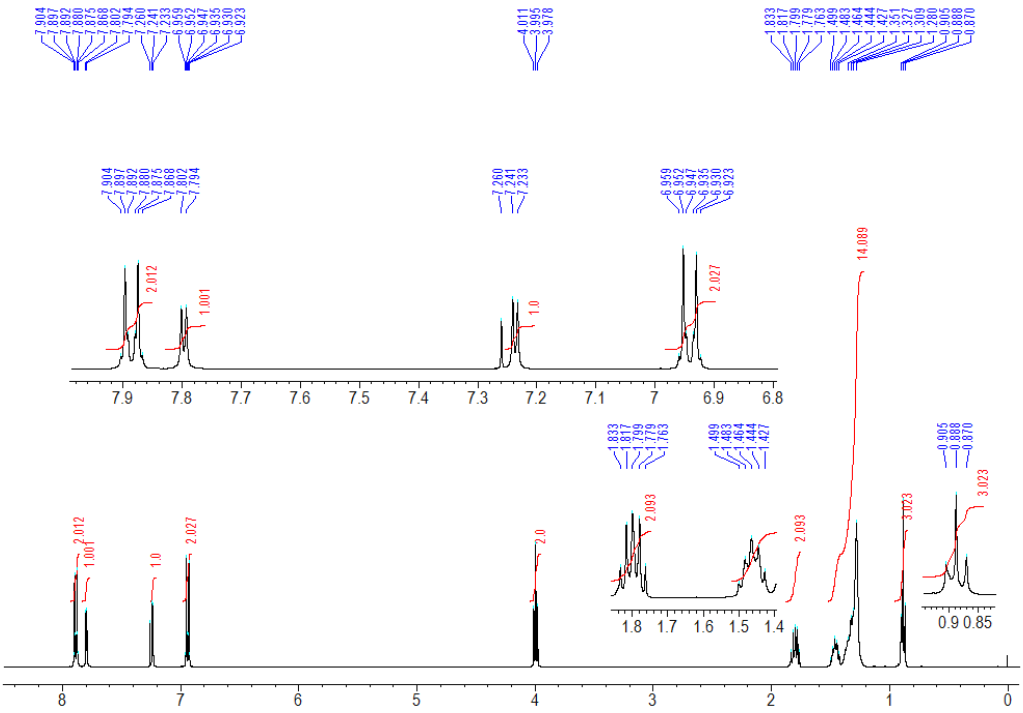

Figure S23. ^{1}H NMR spectrum of **10** in $CDCl_3$ solution (400 MHz).

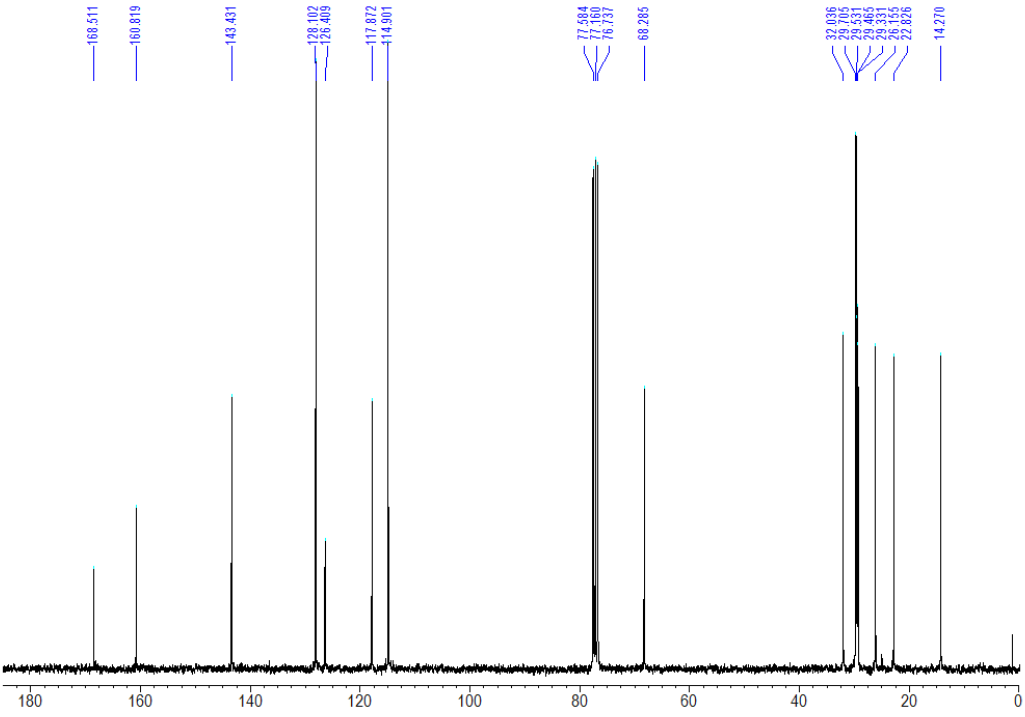

Figure S24. ^{13}C NMR spectrum of **10** in $CDCl_3$ solution (75 MHz).

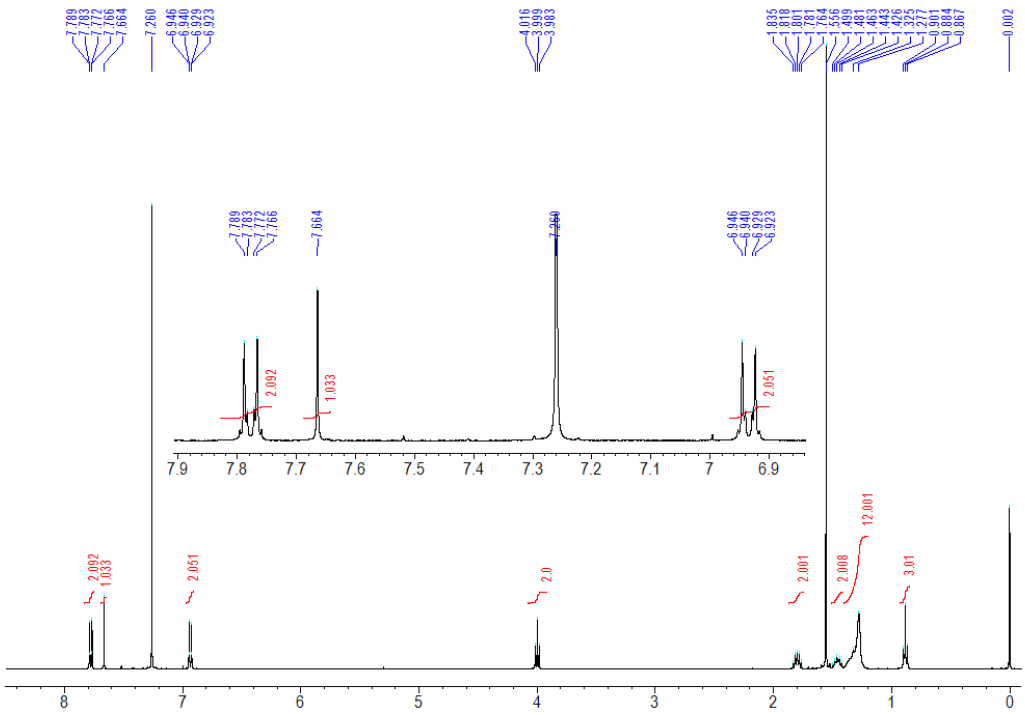

Figure S25. ^{1}H NMR spectrum of **11** in $CDCl_3$ solution (400 MHz).

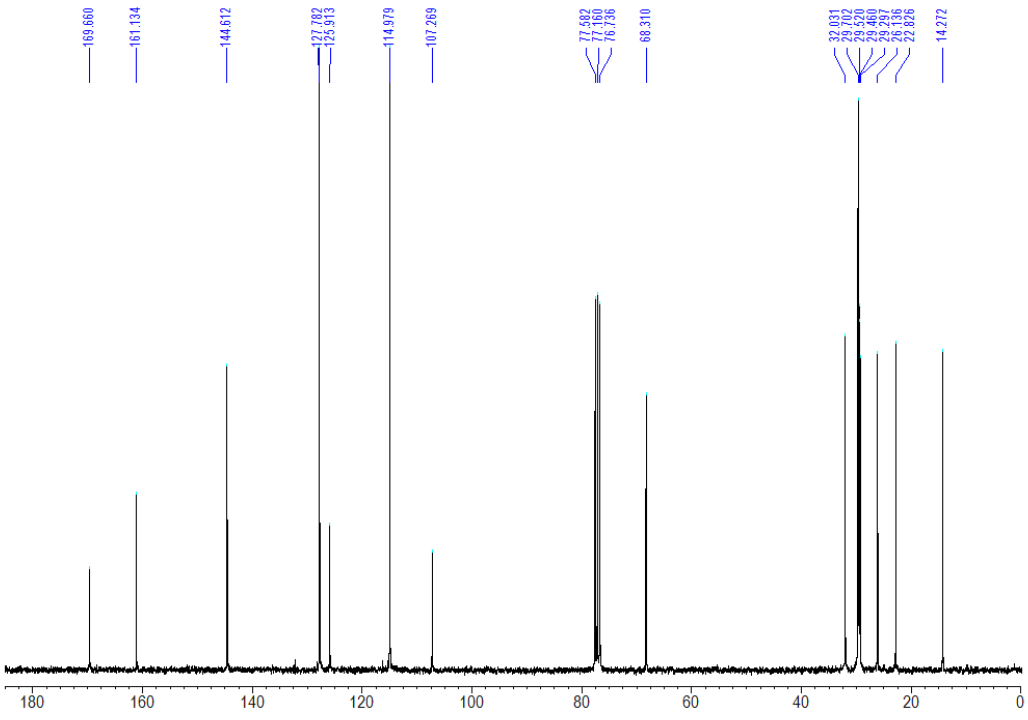

Figure S26. ^{13}C NMR spectrum of **11** in $CDCl_3$ solution (75 MHz).

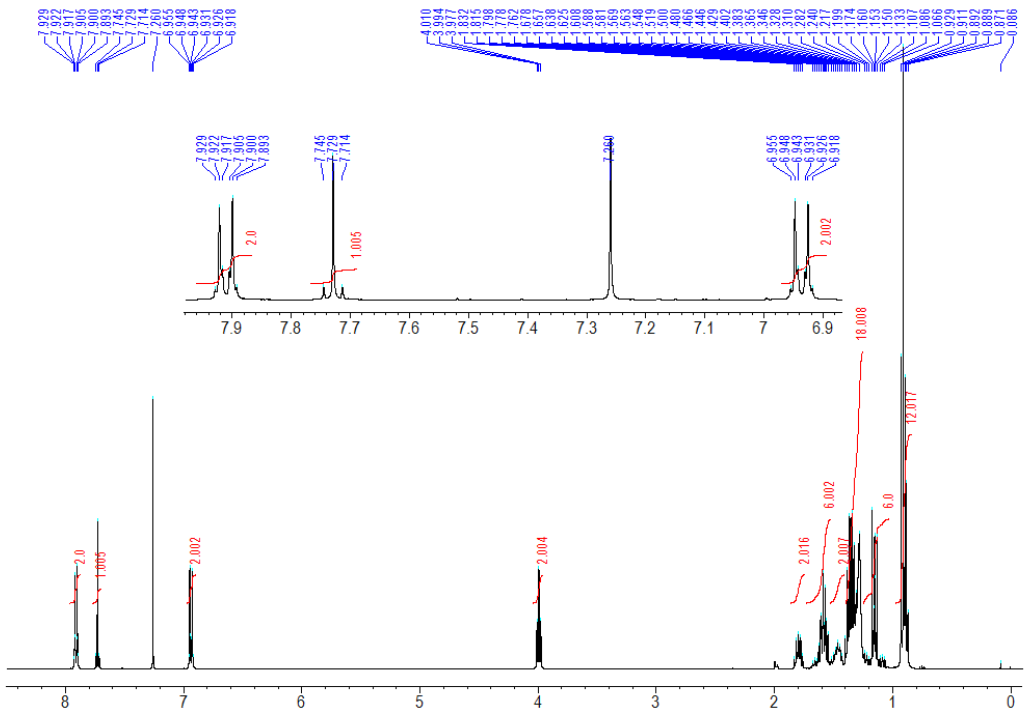

Figure S27. ^{1}H NMR spectrum of **6** in $CDCl_3$ solution (400 MHz).

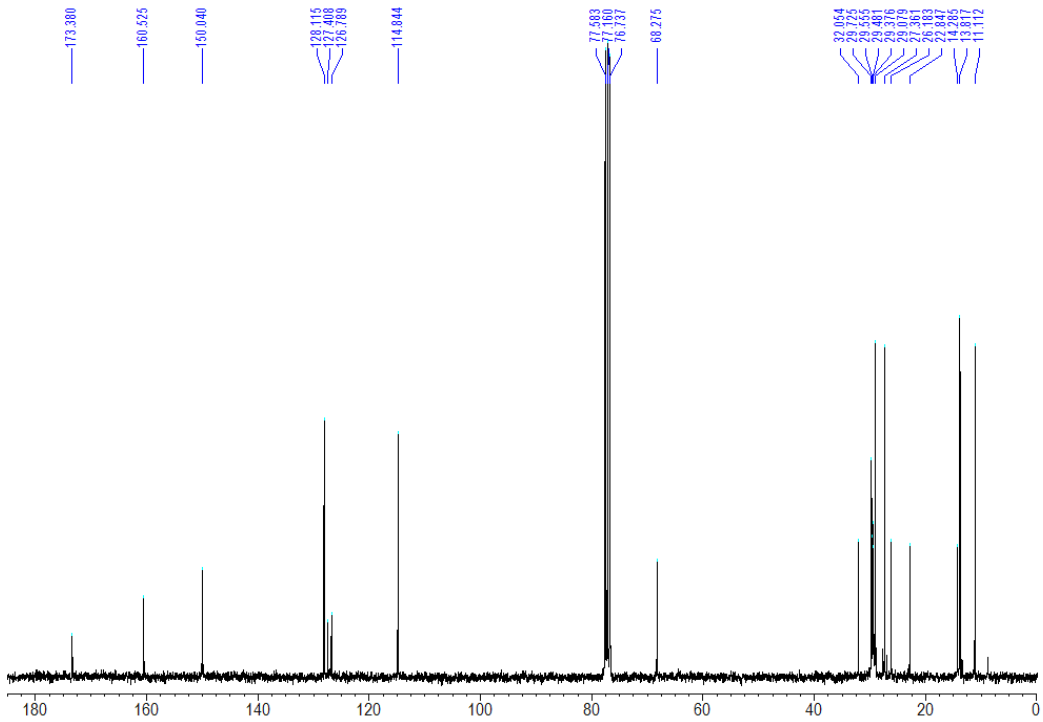

Figure S28. ^{13}C NMR spectrum of **6** in $CDCl_3$ solution (75 MHz).

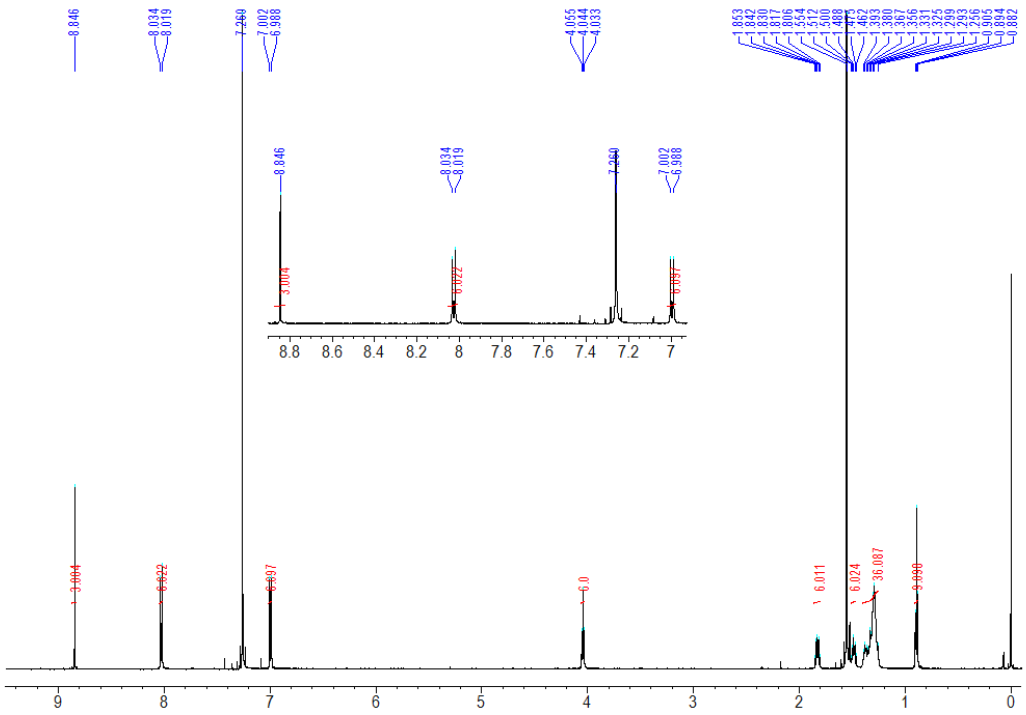

Figure S29. ^{1}H NMR spectrum of **1** in $CDCl_3$ solution (600 MHz).

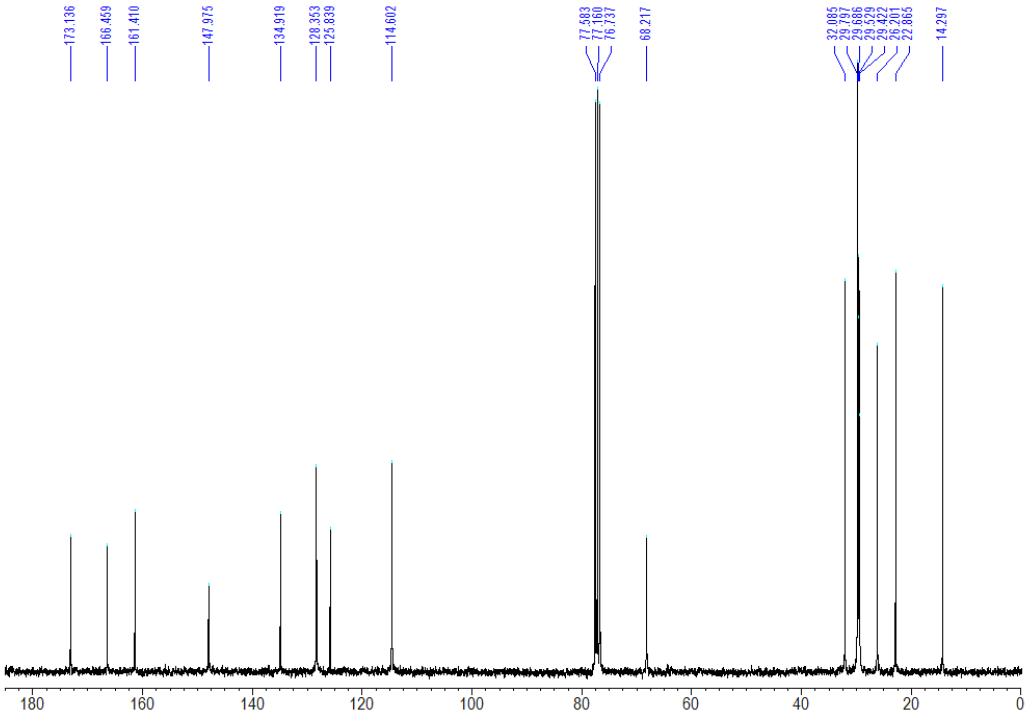

Figure S30. ^{13}C NMR spectrum of **1** in $CDCl_3$ solution (75 MHz).

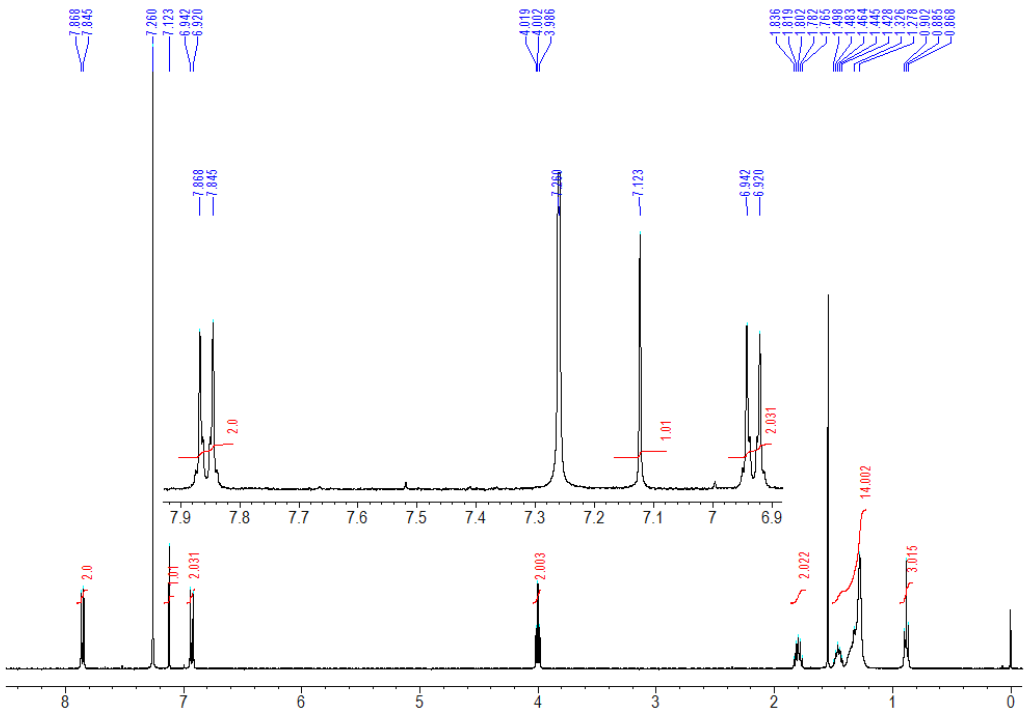

Figure S31. ^{1}H NMR spectrum of **12** in $CDCl_3$ solution (400 MHz).

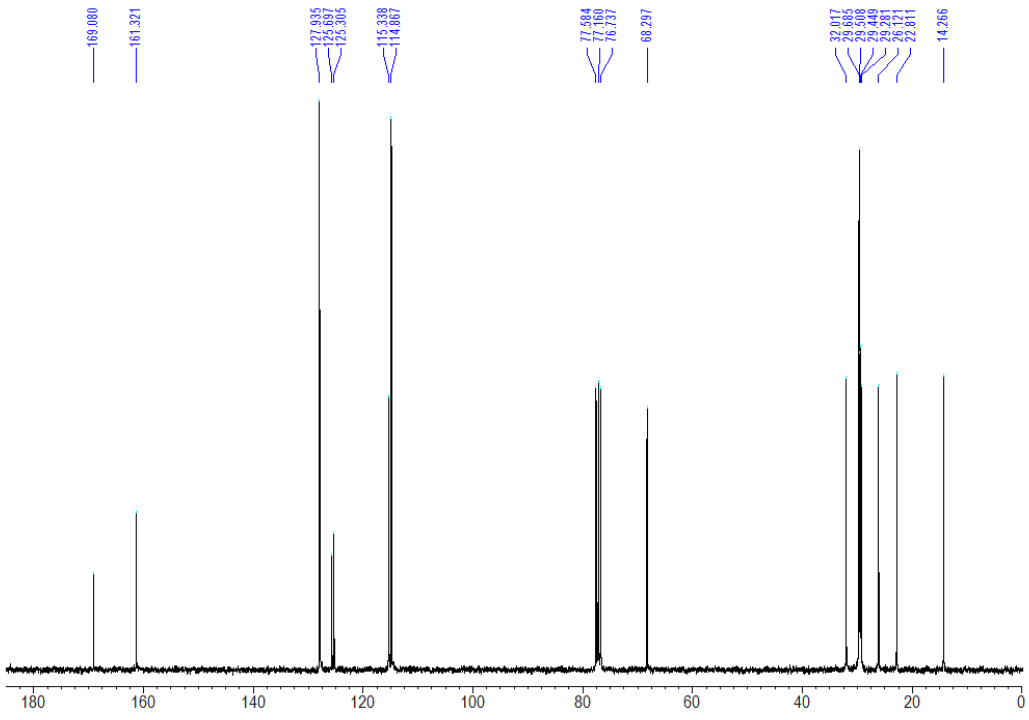

Figure S32. ^{13}C NMR spectrum of **12** in $CDCl_3$ solution (75 MHz).

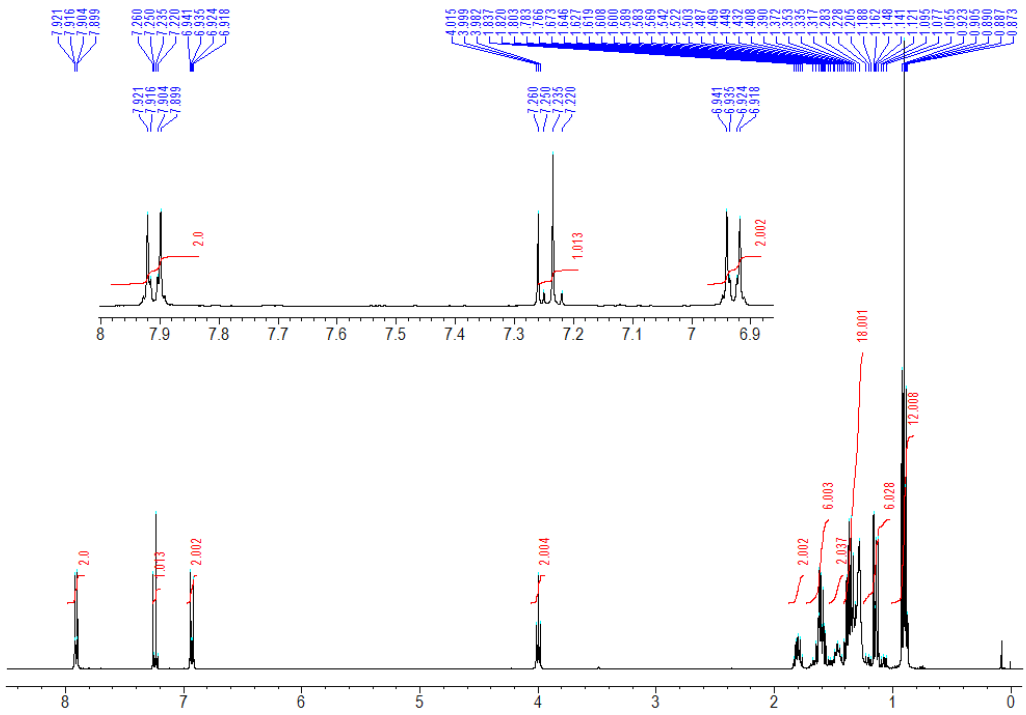

Figure S33. ^{1}H NMR spectrum of **7** in $CDCl_3$ solution (400 MHz).

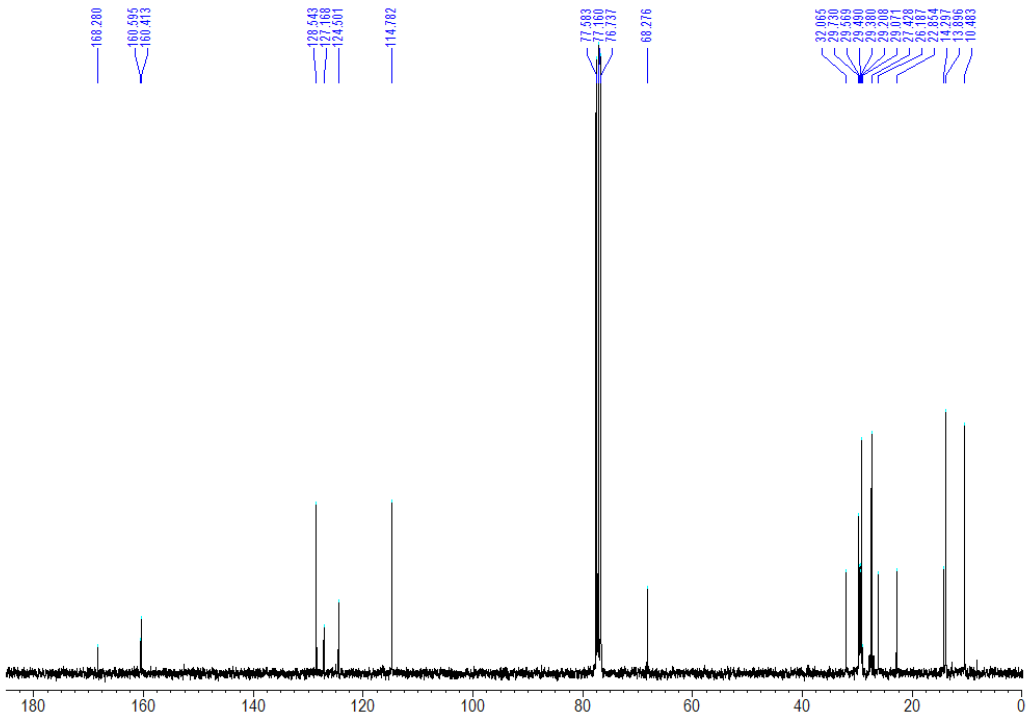

Figure S34. ^{13}C NMR spectrum of **7** in $CDCl_3$ solution (75 MHz).

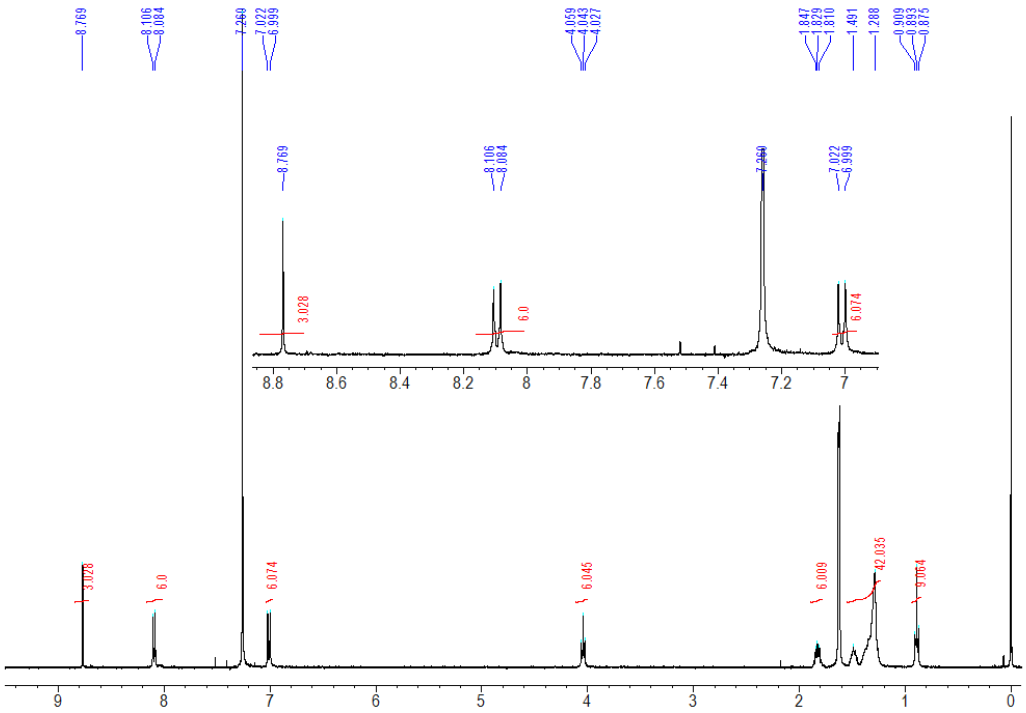

Figure S35. ^{1}H NMR spectrum of **2** in $CDCl_3$ solution (600 MHz).

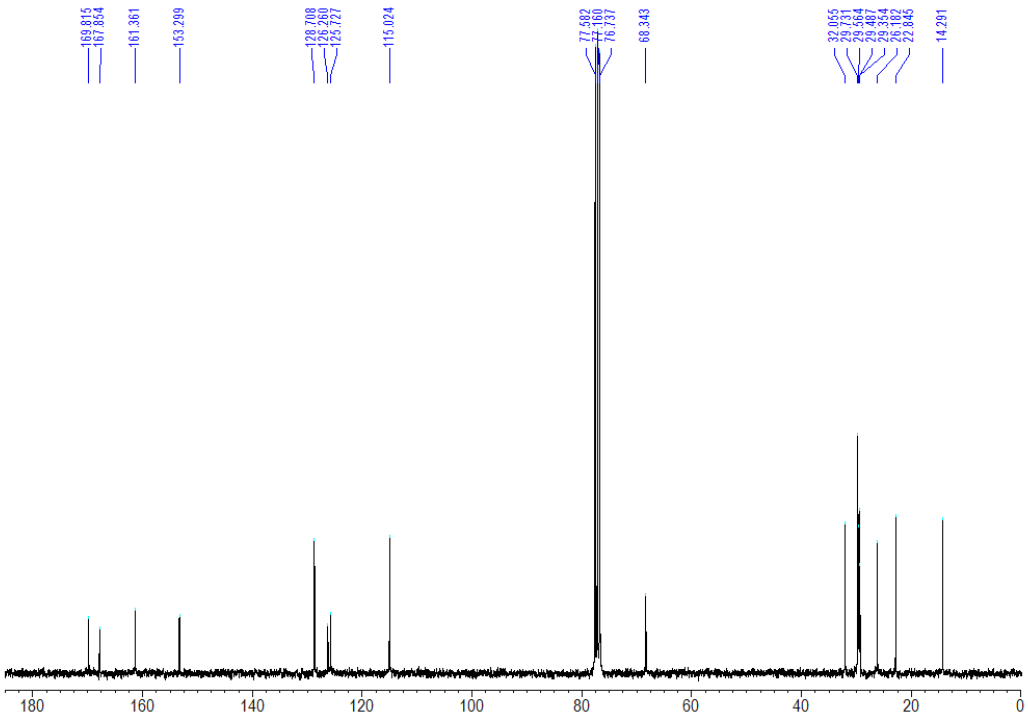

Figure S36. ^{13}C NMR spectrum of **2** in $CDCl_3$ solution (75 MHz).

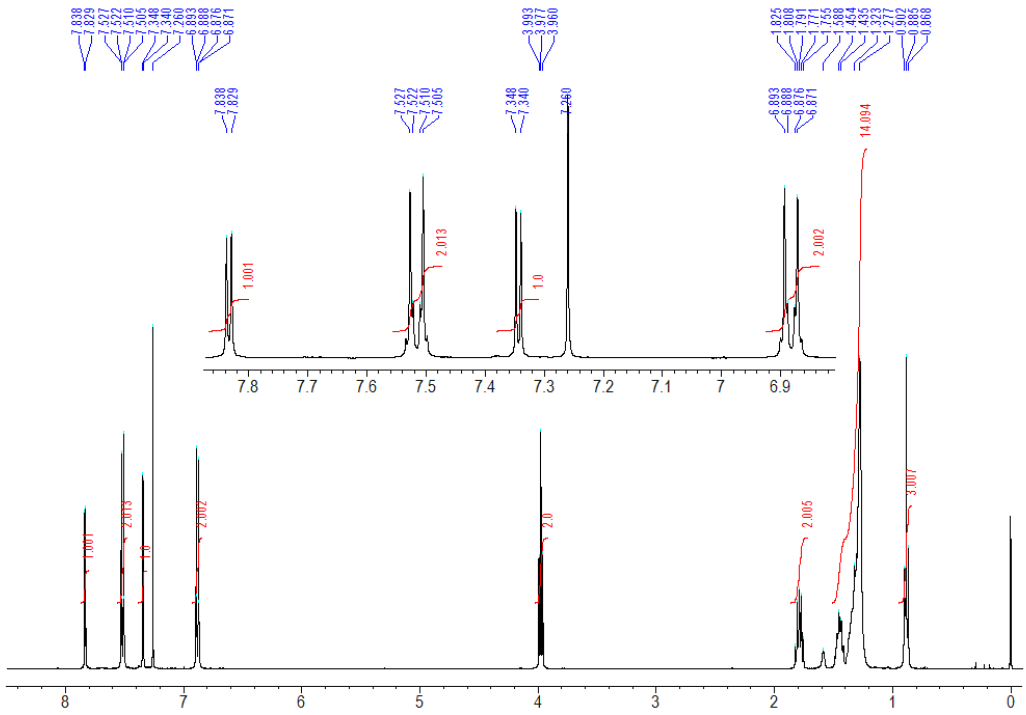

Figure S37. ^{1}H NMR spectrum of **13** in $CDCl_3$ solution (400 MHz).

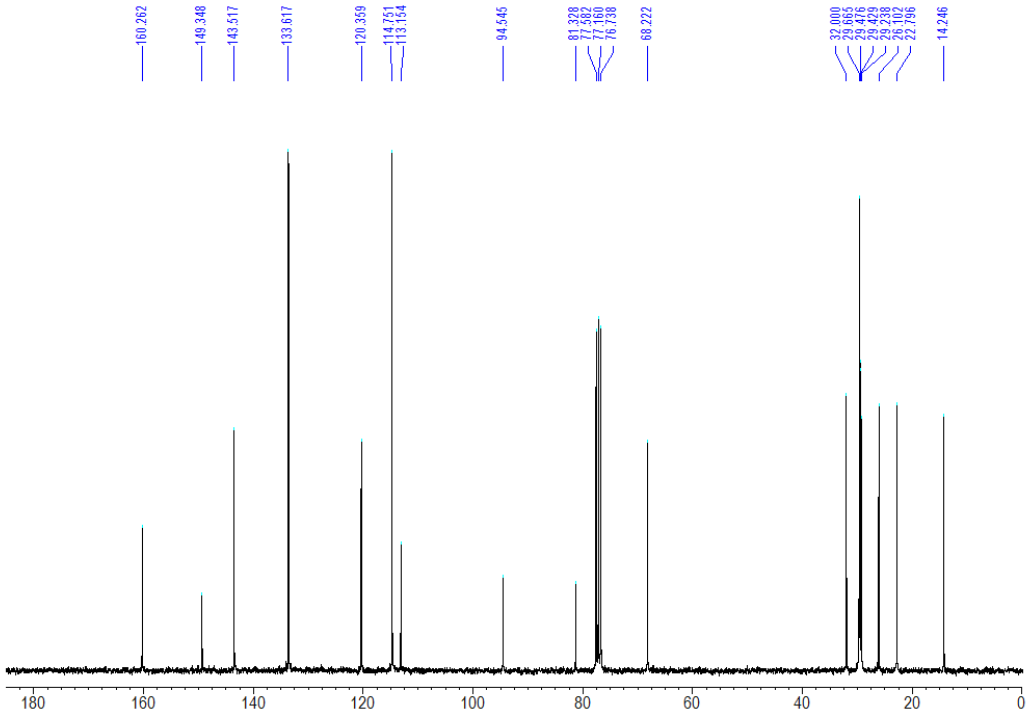

Figure S38. ^{13}C NMR spectrum of **13** in $CDCl_3$ solution (75 MHz).

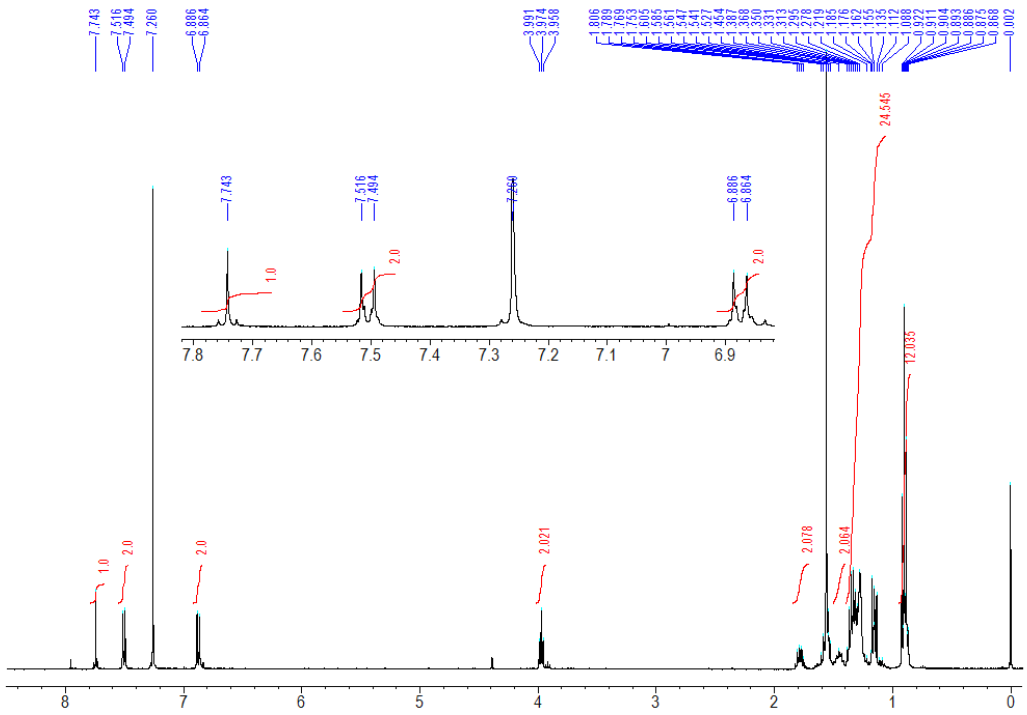

Figure S39. ^{1}H NMR spectrum of **8** in $CDCl_3$ solution (400 MHz).

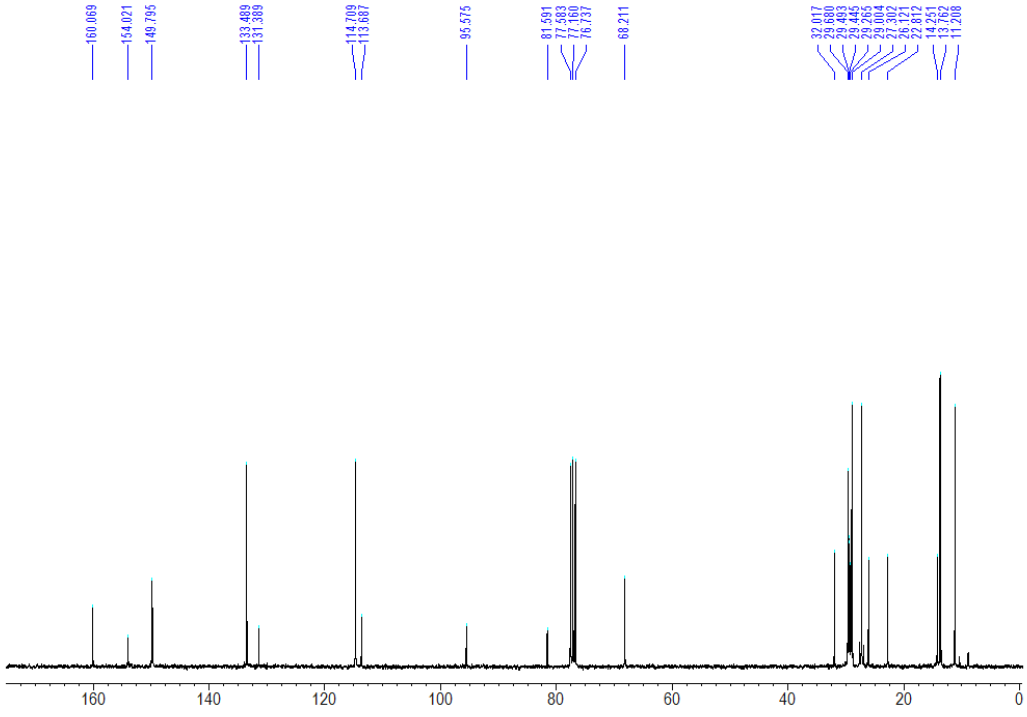

Figure S40. ^{13}C NMR spectrum of **8** in $CDCl_3$ solution (75 MHz).

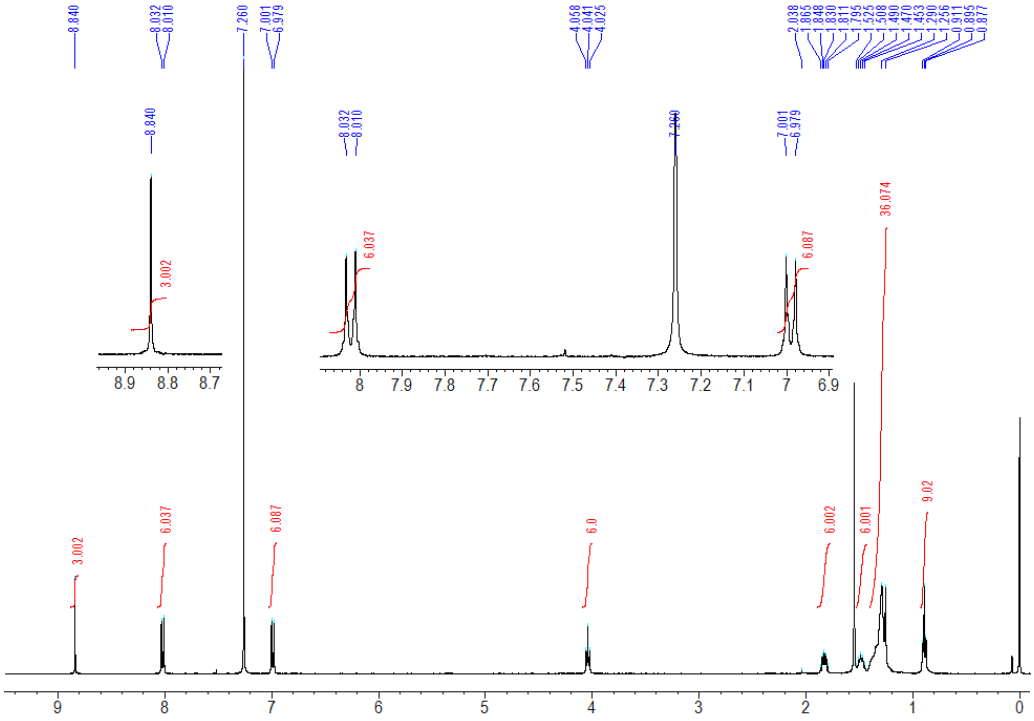

Figure S41. ^{1}H NMR spectrum of **3** in $CDCl_3$ solution (400 MHz).

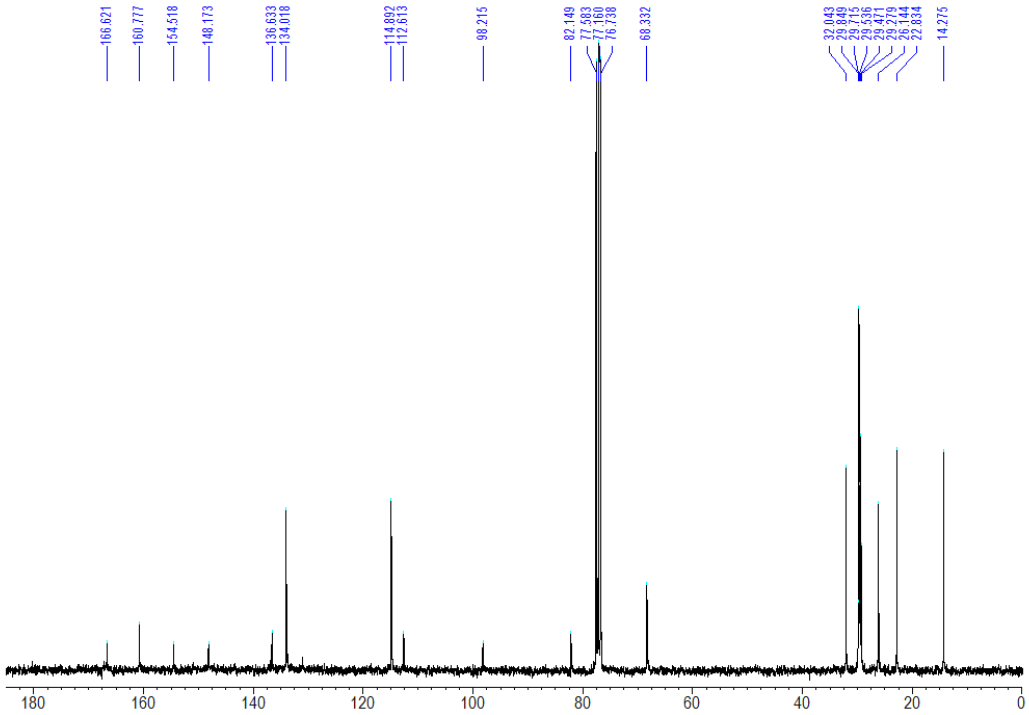

Figure S42. ^{13}C NMR spectrum of **3** in $CDCl_3$ solution (75 MHz).

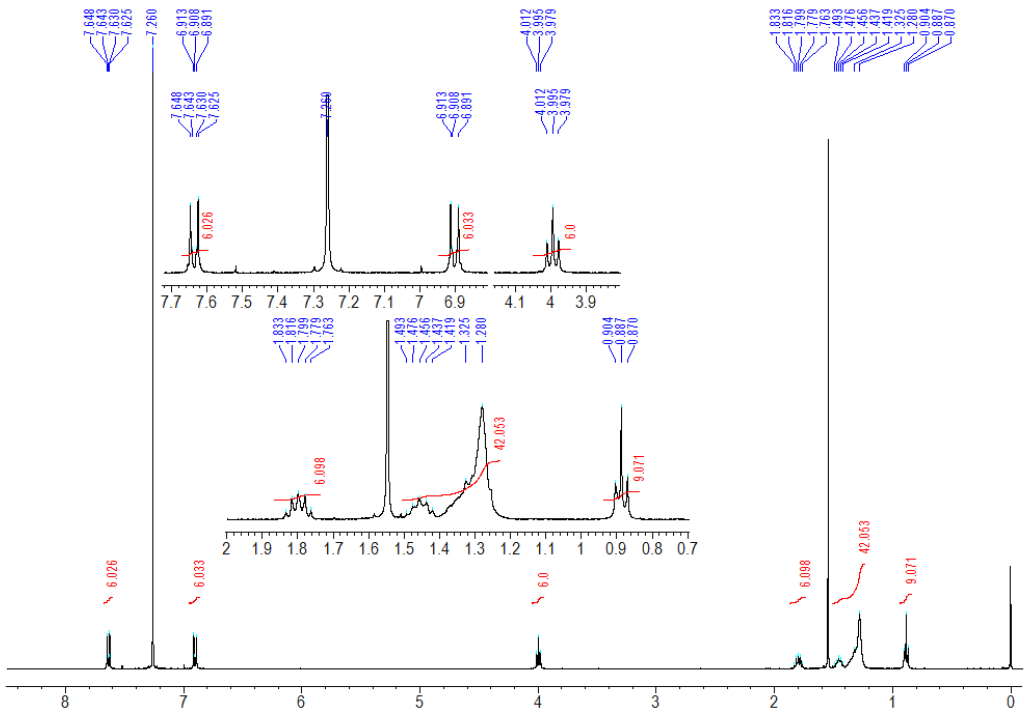

Figure S43. ^{1}H NMR spectrum of **4** in $CDCl_3$ solution (400 MHz).

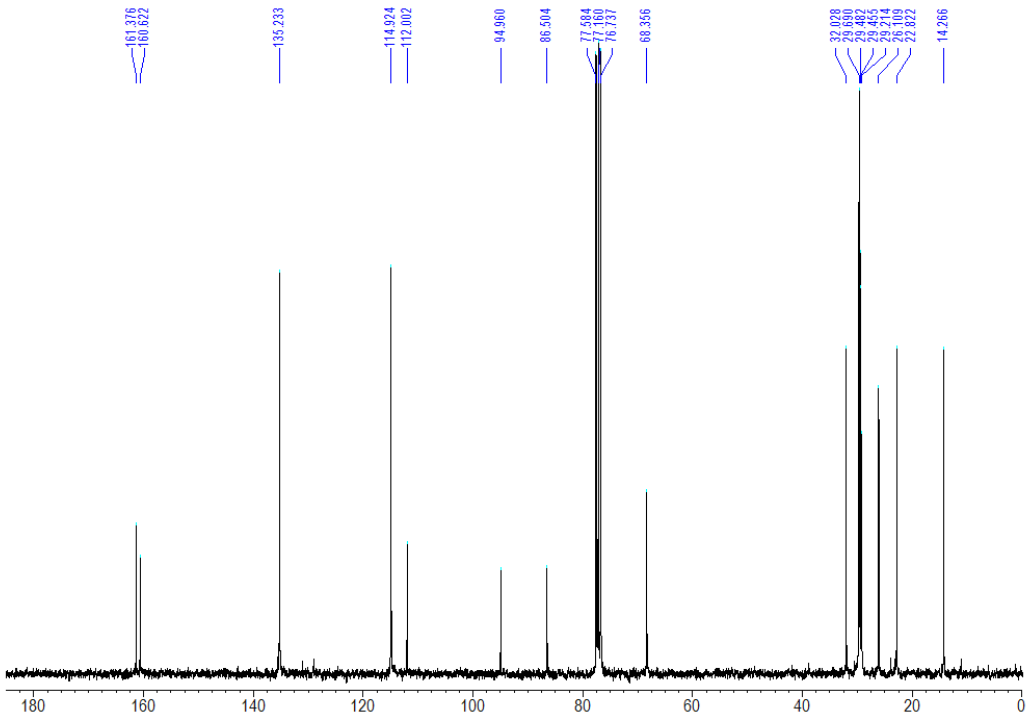

Figure S44. ^{13}C NMR spectrum of **4** in $CDCl_3$ solution (75 MHz).

9. References

1. F. Ozaki, A. Ohashi, N. Uematsu, Patent JPN 2012184223A.
2. J. D. Wood, J. L. Jellison, A. D. Finke, L. Wang, K. N. Plunkett, *J. Am. Chem. Soc.* **2012**, *134*, 15783.
3. A. D. Becke, *Phys. Rev. A* **1988**, 38, 3098-3100.
4. C. Lee, W. Yang, R. G. Parr, *Phys. Rev. B* **1988**, *37*, 785-789.
5. A. D. Becke, *J. Chem. Phys.*, **1993**, *98*, 5648-52.
6. R. Ditchfield, W. J. Hehre, J. A. Pople, *J. Chem. Phys.***1971**, *54*, 724.
7. W. J. Hehre, R. Ditchfield, J. A. Pople, *J. Chem. Phys.* **1972**, *56* 2257.
8. M. E. Casida, C. Jamorski, K. C. Casida, and D. R. Salahub, *J. Chem. Phys.* **1998**, *108*, 4439.
9. S. Grimme, S. Ehrlich and L. Goerigk, *J. Comp. Chem.* **2011**, *32*,1456.
10. F. Weigend and R. Ahlrichs, *Phys. Chem. Chem. Phys.* **2005**, *7*, 3297.
11. S. F. Boys and F. Bernardi, *Mol. Phys.* **1970**, *19*, 553.
12. Gaussian 09, Revision E.12, M. J. Frisch, G. W. Trucks, H. B. Schlegel, G. E. Scuseria, M. A. Robb, J. R. Cheeseman, G. Scalmani, V. Barone, G. A. Petersson, H. Nakatsuji, X. Li, M. Caricato, A. Marenich, J. Bloino, B. G. Janesko, R. Gomperts, B. Mennucci, H. P. Hratchian, J. V. Ortiz, A. F. Izmaylov, J. L. Sonnenberg, D. Williams-Young, F. Ding, F. Lipparini, F. Egidi, J. Goings, B. Peng, A. Petrone, T. Henderson, D. Ranasinghe, V. G. Zakrzewski, J. Gao, N. Rega, G. Zheng, W. Liang, M. Hada, M. Ehara, K. Toyota, R. Fukuda, J. Hasegawa, M. Ishida, T. Nakajima, Y. Honda, O. Kitao, H. Nakai, T. Vreven, K. Throssell, J. A. Montgomery, Jr., J. E. Peralta, F. Ogliaro, M. Bearpark, J. J. Heyd, E. Brothers, K. N. Kudin, V. N. Staroverov, T. Keith, R. Kobayashi, J. Normand, K. Raghavachari, A. Rendell, J. C. Burant, S. S. Iyengar, J. Tomasi, M. Cossi, J. M. Millam, M. Klene, C. Adamo, R. Cammi, J. W. Ochterski, R. L. Martin, K. Morokuma, O. Farkas, J. B. Foresman, and D. J. Fox, Gaussian, Inc., Wallingford CT, 2016.
13. C. A. Hunter, K. R. Lawson, J. Perkins, C. J. Urch, *J. Chem. Soc. Perkin Trans. 2* **2001**, 651.
14. S. Toyota, *Chem. Rev.* **2010**, *110*, 5398.